

Report

**R-19-22**

September 2019



# Phanerozoic faulting of Precambrian basement in Uppland

**Susanne Grigull**

**Gustaf Peterson**

**Johan Nyberg**

**Christian Öhrling**

SVENSK KÄRNBRÄNSLEHANTERING AB

SWEDISH NUCLEAR FUEL  
AND WASTE MANAGEMENT CO

Box 3091, SE-169 03 Solna  
Phone +46 8 459 84 00  
skb.se

SVENSK KÄRNBRÄNSLEHANTERING



ISSN 1402-3091

**SKB R-19-22**

ID 1716952

September 2019

# **Phanerozoic faulting of Precambrian basement in Uppland**

Susanne Grigull, Gustaf Peterson, Johan Nyberg,  
Christian Öhrling

Geological Survey of Sweden

This report concerns a study which was conducted for Svensk Kärnbränslehantering AB (SKB). The conclusions and viewpoints presented in the report are those of the authors. SKB may draw modified conclusions, based on additional literature sources and/or expert opinions.

A pdf version of this document can be downloaded from [www.skb.se](http://www.skb.se).

© 2019 Svensk Kärnbränslehantering AB



## Abstract

The aim of this study is to detect and characterise Phanerozoic faulting of the Precambrian basement for a  $112 \times 112$  km large study area in parts of Uppland and Gästrikland. Bedrock block models are presented based on an updated digital elevation model and an updated model for the depth to bedrock. The area covers both on-shore and off-shore parts. Maximum values for rock block elevation are calculated for each model and relative movement across rock block boundaries, i.e. faults, is detected and characterised. Even though determining the relative timing of fault movement is not possible using the rock block models alone, vertical block displacement is detected mainly across three fault orientations: WNW-ESE and NNE-SSW striking faults with dip slip on the order of tens of meters, and along ENE-WSW striking graben faults around Gävle with a minimum of circa 80 m cumulative slip.

## Sammanfattning

Med syfte att detektera och karaktärisera Fanerozoiska förkastningar i den prekambrisk berggrunden presenteras här berg-block-modeller baserade på en uppdaterad digital höjdmodell och en uppdaterad jorddjupsmodell (dvs. djup till berg). Det undersökta området är  $112 \times 112$  km stort och täcker både terrestra och marina delar av Uppland och Gästrikland. Förkastningar har karaktäriserats med hjälp av beräkningar av maximala berg-block-höjder för respektive modell, och de relativa rörelserna har bestämts mellan blockgränserna. Även om det inte är möjligt att datera relativa förkastningsrörelser med denna metod, så har blockrörelser detekterats utmed tre huvudsakliga förkastningsriktningar: VNV–OSO och NNO–SSV med relativa vertikala blockrörelser på tiotals meter, samt utmed ONO–VSV strykande graben-förkastningar i Gävleområdet med kumulativa rörelser på minst cirka 80 m.

# Contents

<b>1</b>	<b>Introduction</b>	7
<b>2</b>	<b>Geological framework</b>	9
2.1	Svecokarelian orogeny	9
2.2	Post-Svecokarelian geological evolution	12
<b>3</b>	<b>Methodology</b>	15
3.1	Base data	15
3.2	Lineament interpretation and rock block boundaries	16
3.3	Depth to bedrock and bedrock elevation relative to sea level	19
3.4	Correction for topographic gradient	21
<b>4</b>	<b>Results</b>	23
4.1	Maximum rock block elevation	23
<b>5</b>	<b>Discussion</b>	27
5.1	Interpolation of trend surface for removal of topographic gradient	27
5.2	Relative block movement	27
5.3	Relative fault timing based on lineament abutting relationships	30
5.4	Rock block model limitations	30
<b>6</b>	<b>Conclusions</b>	33
	<b>Acknowledgements</b>	35
	<b>References</b>	37





# 1 Introduction

The aim of this study is to detect and characterize vertical displacements of bedrock blocks in the Uppland and Gästrikland area, which includes the site of a planned nuclear waste repository at Forsmark (Figure 1-1). This is done using a digital elevation model (DEM) of the bedrock surface that lies beneath the Quaternary sedimentary cover and extends beneath present sea level. From this DEM a rock block model for a  $112 \times 112$  km large area is produced and is used to calculate metrics that may indicate potential movements of the rock blocks relative to each other after formation of a key regional unconformity, the so-called sub-Cambrian peneplain.

The morphology of the present bedrock surface, locally covered by Quaternary glacial deposits, is generally thought to reflect glacial erosion acting on the structural inventory of the bedrock of the Fennoscandian shield. In particular localised, brittle deformation zones, with high fracture densities, can correspond to topographic minima in height models. Depending on the studied scale, the mapped length of these zones can vary (tens of meters to hundreds of kilometres), and what seems like one long deformation zone at a small scale may actually be composed of several shorter zones at a large scale. Independent of the scale, a property common to all these zones is their high length-to-width aspect ratio making them appear as thin linear morphological features that can be traced as lineaments in topographic models (Hobbs 1903, 1912; see also Tirén 2010).

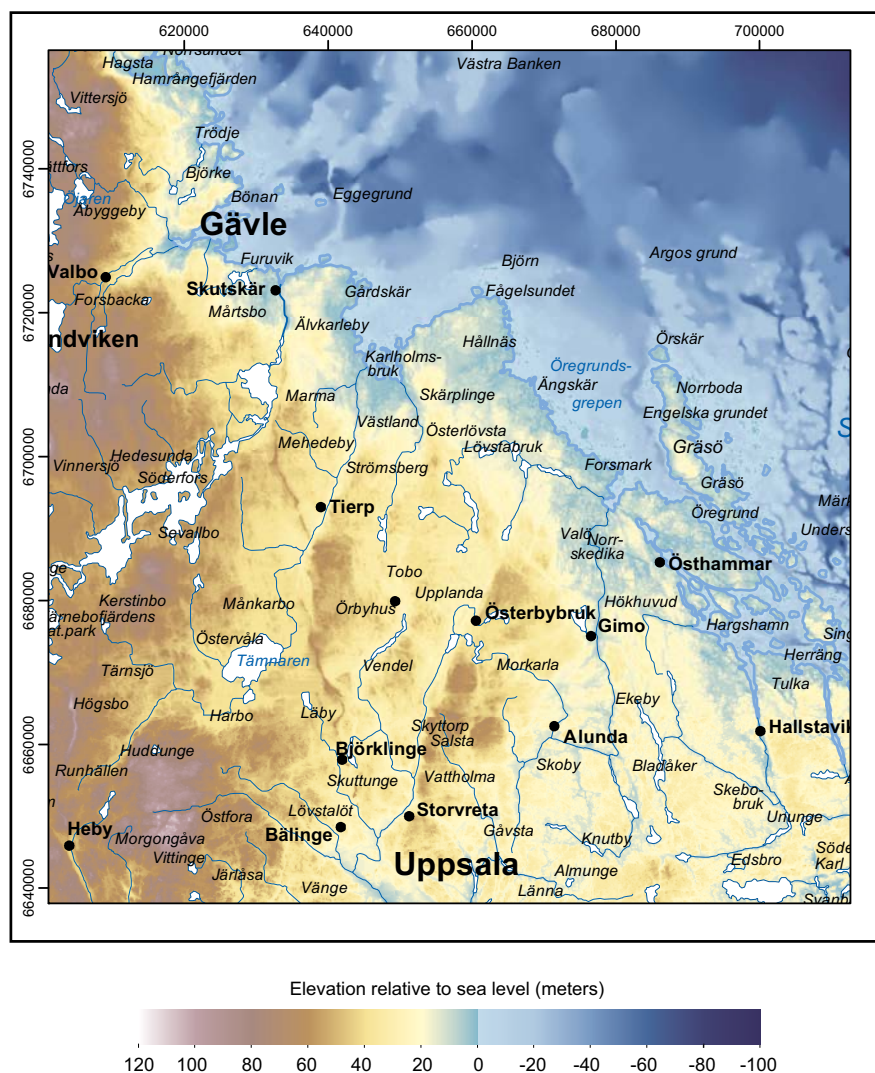


**Figure 1-1.** Overview map with on-shore elevation and bathymetry of the study area. Raster resolution is  $50 \times 50$  m. Coordinates are in meters (SWEREF99TM).

Rock blocks are defined as areas of the bedrock surface that are bounded by such lineaments. Block size depends entirely on the working scale. Differences in the elevation of such rock blocks can indicate differential vertical displacement of the bedrock surface. A method to produce rock block models based on elevation data is presented by e.g. Tirén and Beckholmen (1992) and in several reports by the Swedish Radiation Safety Authority (Strålsäkerhetsmyndigheten) by the same authors (e.g. Beckholmen and Tirén 2010a, b). The work presented in the current report is an improvement of the previous studies since it applies a bedrock surface model, instead of a land surface model, to detect block displacements. Further, the bedrock surface model is based on an up-to-date LiDAR derived digital elevation model, bathymetry, and an updated depth-to-bedrock model. Different methods to detrend the pre-Cambrian reference plane are also explored. The current study has applied the method of Beckholmen & Tirén. The base data and work flow are presented in the section labelled 'Methodology'.

## 2 Geological framework

The bedrock of the study area and the fracture networks therein reflect more than 1.9 billion years of Earth history (Figure 2-1), which is briefly summarized below. More detailed information on the geological history of the area can be found in numerous publications (e.g., Lidmar-Bergström 1994, Hermansson et al. 2007, Söderbäck 2008, Högdahl et al. 2009, Stephens et al. 2009, Saintot et al. 2011, Stephens et al. 2015).

### 2.1 Svecokarelian orogeny

The rocks in the study area belong to the Bergslagen lithotectonic unit of the Fennoscandian Shield (Figure 2-2). This unit is bounded by the Loftahammar-Linköping zone to the south and the Hagsta-Storsjön-Edsbyn zone to the north (e.g. Högdahl et al. 2009, Curtis et al. 2018 and references therein). Magmatic intrusive and supracrustal volcanic rock suites and clastic metasedimentary rocks dominate the on-shore part of the area (Figure 2-3). These rocks formed and were deformed between c. 1.9 and 1.8 Ga during the Svecokarelian orogeny (e.g. Stephens et al. 2009, Stephens 2010, Stephens et al. 2015 and Figure 2-1). After 1.8 Ga, tectonic activity in the Svecokarelian orogen waned and late- and post-orogenic granites and pegmatites were intruded between 1.85–1.75 Ga. Brittle deformation continued during this period up to the intrusion of magmatic rocks at c. 1.7–1.67 Ga in western Bergslagen (e.g. Stephens 2010 and Figure 2-1).

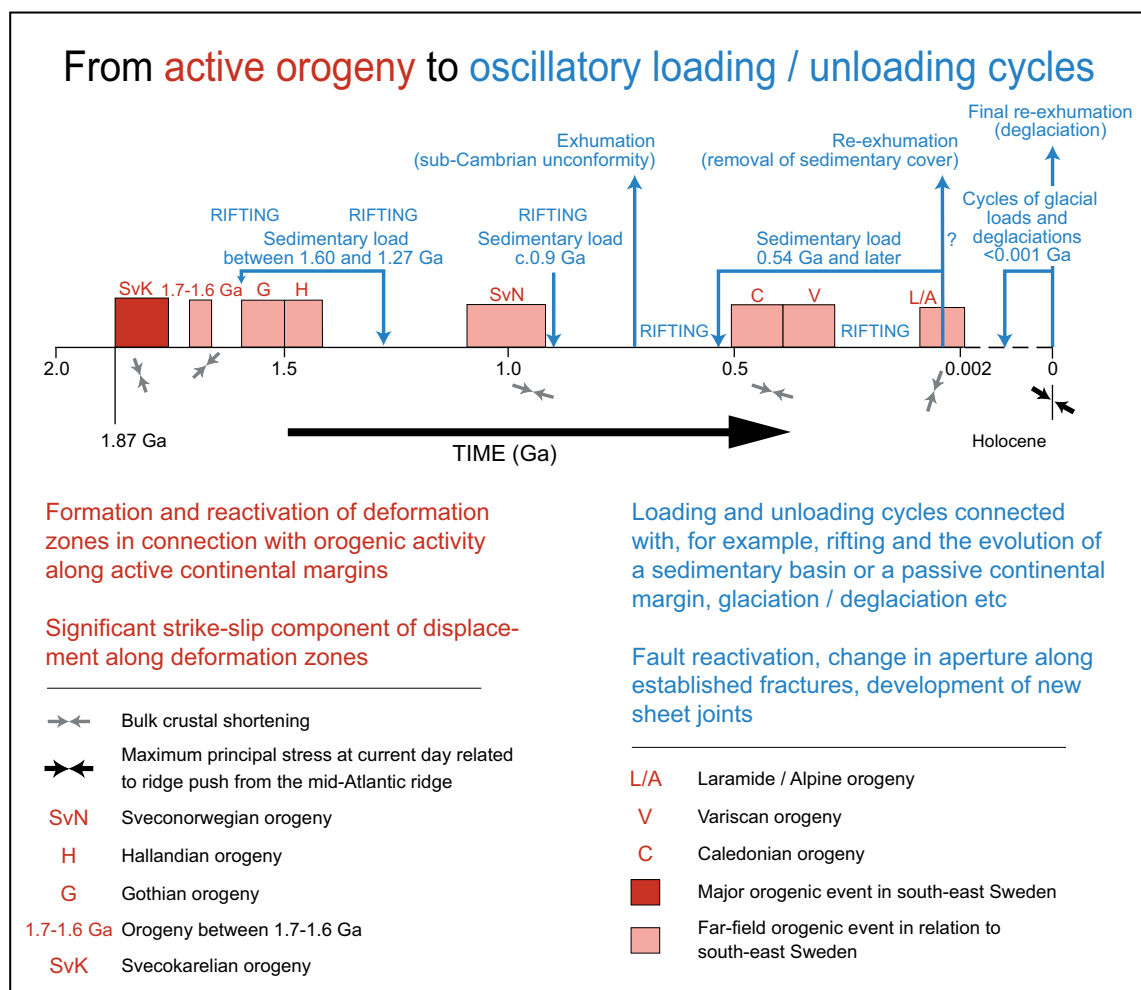


**Figure 2-1.** Schematic diagram showing tectonic evolution from ca. 1.9 Ga to present. Figure taken from Stephens (2010).

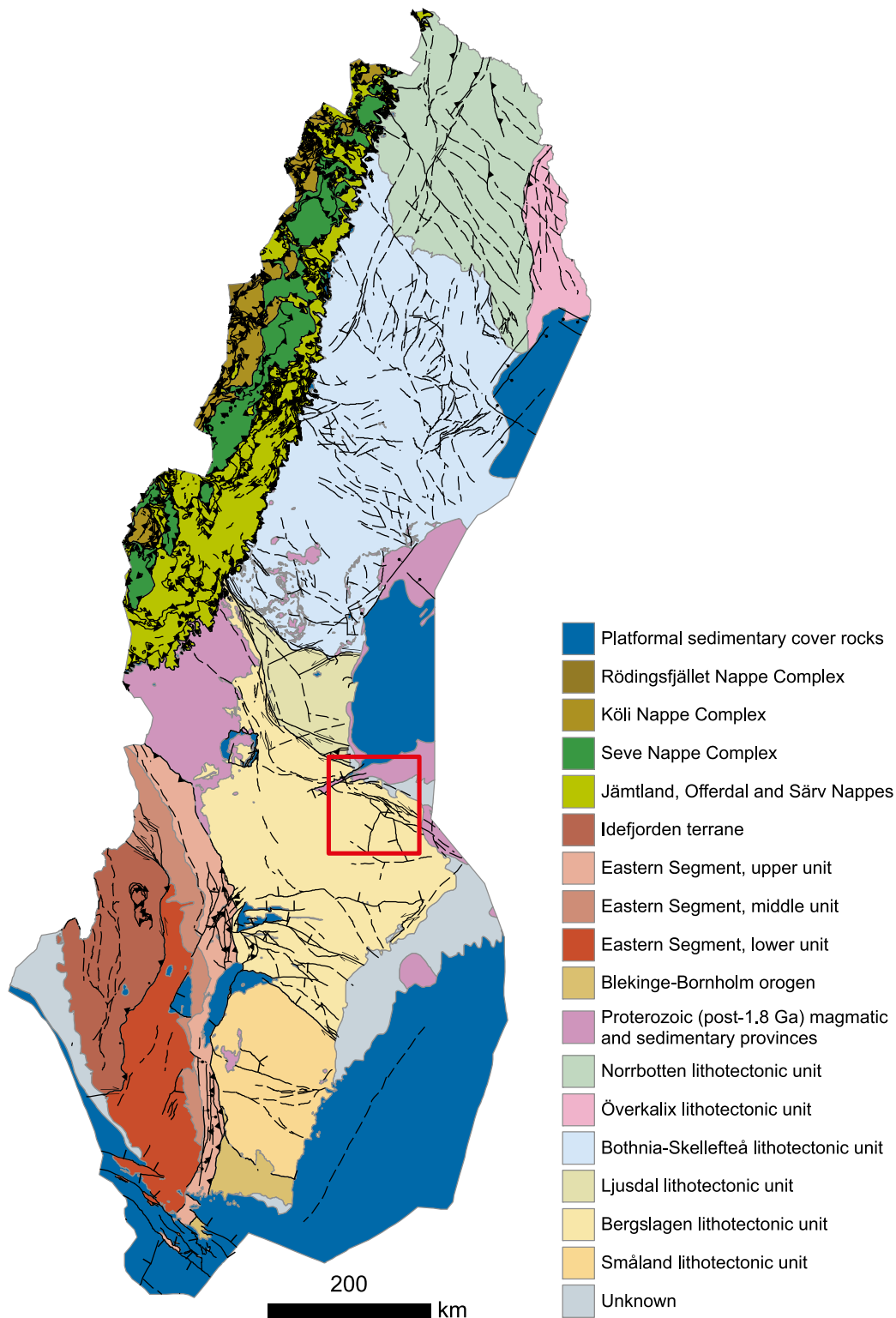


**Figure 2-2.** Lithotectonic units in Sweden (Based on Bergman et al. (2012)). Red box indicates location of study area.

Multi-phase ductile deformation and metamorphism affected the Bergslagen unit during the Svecokarelian orogeny (Stephens et al. 2009 and references therein). Ductile high strain belts striking WNW-ESE to NW-SE provide the precursor to WNW-ESE to NW-SE striking, steeply dipping ductile to brittle-ductile, dextral strike-slip shear zones such as the Singö and Forsmark deformation zones which occur along the northeastern coast of Uppland (Figure 2-3). The NNE-SSW and N-S striking shear zones, such as the Österbybruk-Skyttorp (ÖSZ) and the Gimo deformation zones (Figure 2-3) are the result of a complicated poly-phase deformation process in the ductile and brittle-ductile field.

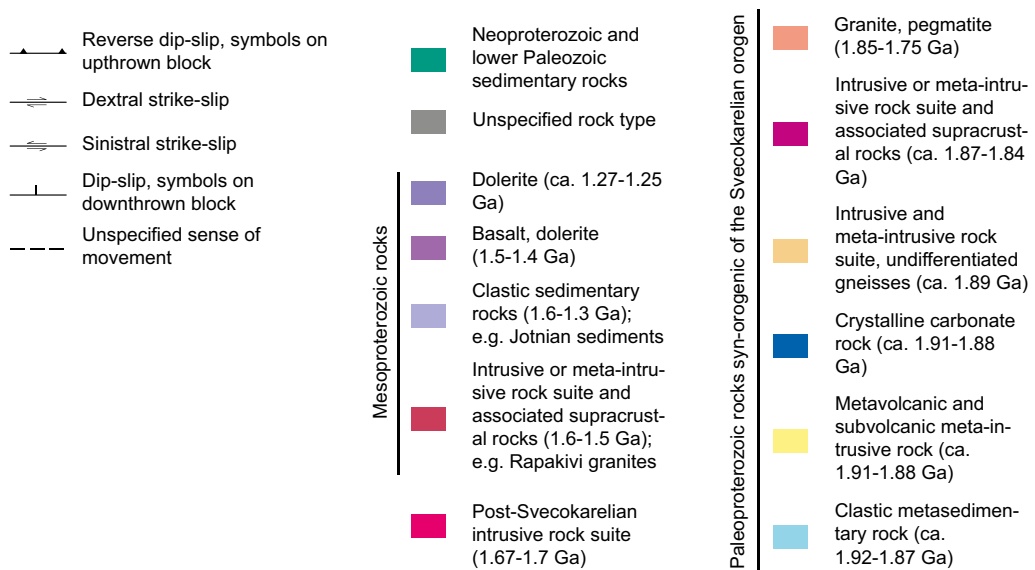
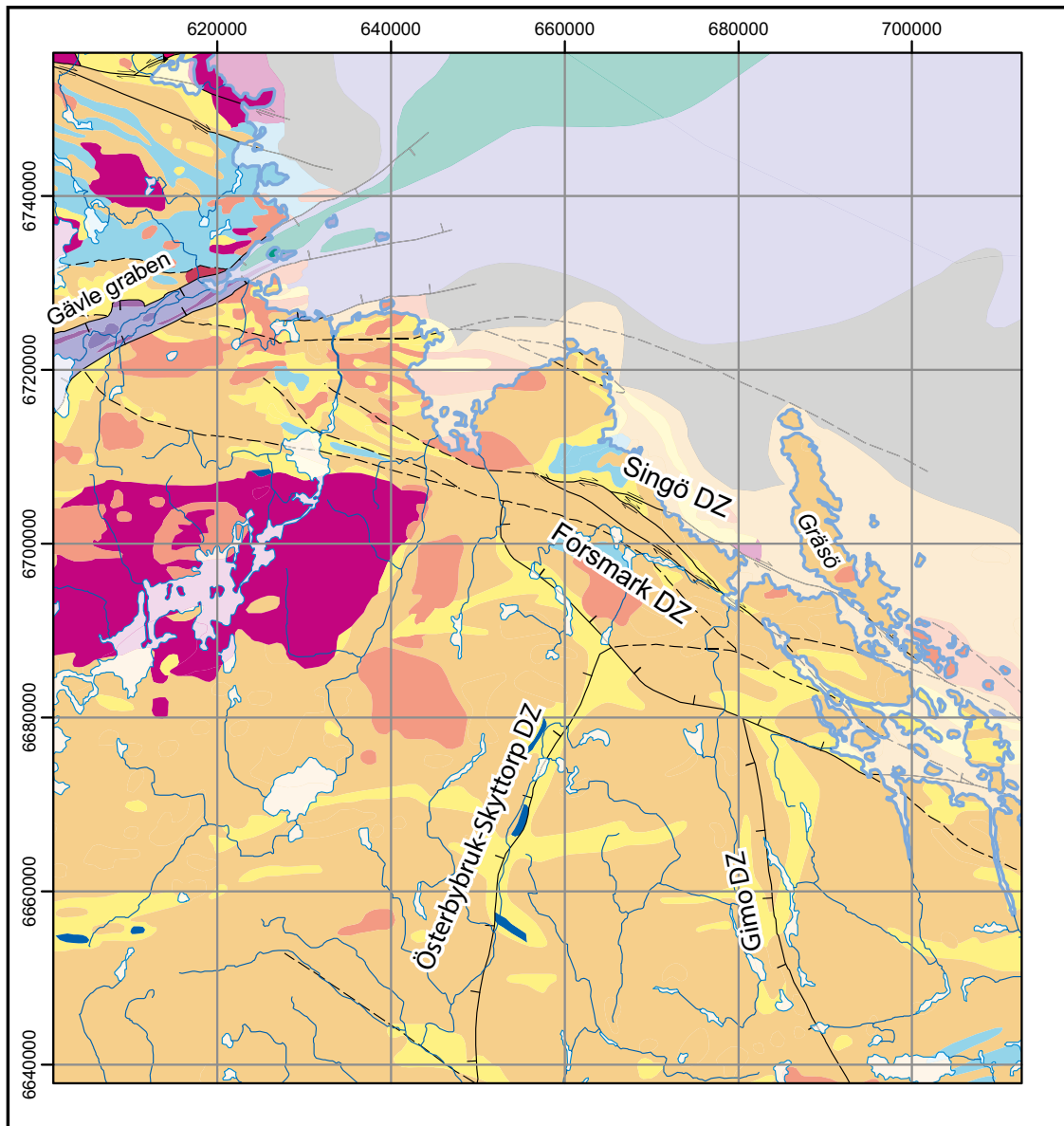


**Figure 2-3.** Bedrock map of the study area situated in the Bergslagen lithotectonic unit. Based on Bergman et al. (2012) and Stephens et al. (2009). Coordinates are in meters (SWEREF99TM).

They are interpreted to have initially formed as ductile high-strain envelopes to tectonic lenses. During the evolution of the Singö shear zone system, progressive shearing and pinning by the intrusion of 1.8 Ga granites is then thought to have led to rotation of the ductile shear zones into their current position (Persson and Sjöström 2003, Högdahl et al. 2009). Seismic imaging of the Österbybruk-Skyttorp deformation zone shows that mylonites of the ÖSZ dip to the east and structural geological studies indicate dextral, eastern-side-up kinematics during the last ductile shearing phase (Persson and Sjöström 2003, Högdahl et al. 2009, Malehmir et al. 2011).

## 2.2 Post-Svecokarelian geological evolution

The Bergslagen unit was influenced by far-field tectonic stresses during 1.7–1.6 Ga. During this period, the WNW-ESE striking shear zones were reactivated as sinistral shear zones in the brittle field by NE-SW-directed transpression (Saintot et al. 2011, Stephens et al. 2015). During the Mesoproterozoic (1.6–1.0 Ga), tectonic activity shifted to active margins in southern and southwestern Sweden during the Gothian (1.66–1.52 Ga) and Hallandian (1.47–1.38 Ga) orogeny (Bingen et al. 2008, Stephens et al. 2015) with potential far-field responses such as weak extension in the Bergslagen region (e.g. Ahl et al. 1997, Bingen et al. 2008). Extension is expressed by the intrusion of the Rapakivi granite suites around 1.5 Ga in Bergslagen (e.g. Ahl et al. 1997), graben formation and deposition of clastic sediments such as the so-called Jotnian sedimentary rocks in these grabens (e.g. Sederholm 1897, Gorbatshev 1967, Amantov et al. 1996, Lidmar-Bergström 1996, Stephens et al. 2015 and references therein). The Jotnian sedimentary rocks are dominantly fluvial and subaerial deposits and are estimated to have been deposited between 1.6 and 1.26 Ga onto a sub-Jotnian denudation surface (Amantov et al. 1996, Lidmar-Bergström 1996). In the study area, the Jotnian sedimentary units are partially bound by faults forming the Gävle graben (Figure 2-3), which strike WSW-ENE under the Bothnian Sea (Figure 2-3, see also Ahlberg 1986, Lidmar-Bergström 1996). The present maximum thickness of the Jotnian sedimentary units is estimated to be 900–1 000 m (Gorbatshev 1967, Winterhalter 1972). During initial rifting of the Gävle graben, the Jotnian sedimentary units were intruded by Mesoproterozoic basaltic rocks aged c. 1.48–1.46 Ga, thereby constraining the deposition of the Jotnian sediments to at least this age. A second rifting phase is indicated by 1.27–1.26 Ga dolerite dykes that also intruded the Jotnian sedimentary rocks in the Gävle graben (e.g. Elming and Mattsson 2001 and Figure 2-3). Jotnian outliers also are found in the archipelago W of Singö (Söderberg and Hagenfeldt 1995).

During the Sveconorwegian orogeny (1.1 to 0.9 Ga, Figure 2-1), E-W to WNW-ESE oriented bulk crustal shortening reactivated the older WNW-ESE striking deformation zones, which renewed sinistral movement along e.g. the Singö deformation zone (Stephens et al. 2007, 2015, Saintot et al. 2011).

During the late Neoproterozoic, after the Sveconorwegian orogeny, but before the Cambrian transgression, the crystalline basement of the Fennoscandian shield and the Jotnian sedimentary cover rocks were eroded to an extensive low relief surface, labelled the sub-Cambrian peneplain (Lidmar-Bergström 1994, see also Figure 2-4). Palaeozoic and younger sedimentary rocks were deposited on the peneplain (Larson et al. 1999, Cederbom 2001, Stephens and Wahlgren 2008, Lidmar-Bergström and Olvmo 2015, Stephens et al. 2015). (U-Th)/He apatite ages from surface and subsurface samples in crystalline bedrock around Forsmark indicate that the Paleozoic and younger cover rocks had a thickness of 3 km during the Silurian (Söderbäck 2008). By the Early Jurassic, the sedimentary cover was still greater than 2 km which may have prevented the sub-Cambrian peneplain in the study area from undergoing deep Mesozoic weathering as is observed elsewhere in Sweden (Lidmar-Bergström 1995, Larson et al. 1999, Cederbom 2001, Stephens and Wahlgren 2008, Lidmar-Bergström and Olvmo 2015, Stephens et al. 2015). Re-exhumation of the sub-Cambrian peneplain did probably not occur until the Cenozoic (Söderbäck 2008) or even Pleistocene (Hall et al. 2019).

In the Öregrundsleden, fault-bound outliers of Early Ordovician limestone are interpreted to rest directly on basement (Söderberg and Hagenfeldt 1995). This indicates erosion and depositional breaks during the Cambrian and Ordovician and syn- to post-Ordovician faulting. Further, Phanerozoic fracturing and faulting of the sub-Cambrian peneplain and its cover rocks is indicated by faulted Lower Paleozoic rocks in the Gävle graben and in the Åland Sea (Söderbäck 2008 and references therein). Also, brittle reactivation of the Österbybruk-Skyttorp deformation zone and zones that are subparallel to the ÖSZ displaced adjacent blocks of the sub-Cambrian peneplain with west-side-down kinematics (Persson and Sjöström 2003). It is unclear whether these kinematics indicate brittle reactivation in an extensional regime which would have caused normal faulting along the ÖSZ and parallel shear zones or reactivation in a compressional regime, which would have caused reverse faulting (see discussion). The timing of this reactivation is also unclear.

<sup>40</sup>Ar/<sup>39</sup>Ar-dating of generation 3 adularia (Sandström et al. 2006) resulted in an age of  $276.9 \pm 1.1$  Ma in a NE-SW striking, steeply dipping fracture (039/84) at 245.47 m depth in drill core KFM08A (N6700320.43, E675479.821) near Forsmark and indicates brittle deformation in the area even during the Permian. It is unclear to what extent the Caledonian, Variscan and Alpine orogenies (Figure 2-1) affected and disturbed the sub-Cambrian peneplain. Phanerozoic brittle faulting of the sub-Cambrian peneplain and overlying early Ordovician sediments is reported also from other locations in southern Sweden (e.g. Tirén and Beckholmen 1989, Munier and Talbot 1993, Johansson 1999).

During the Quaternary, the area around Forsmark was repeatedly covered by ice sheets that were up to 3 km-thick during glacial maxima (e.g. Näslund 2010). The advance and retreat of these ice sheets over the landscape may have reactivated existing shallowly dipping fractures (sheeting joints), which are locally filled with glacial sediments (Carlsson 1979, e.g. Leijon 2005 and references therein, Lönnqvist and Hökmark 2013). Sheeting joints usually occur to a depth of several tens of meters and run sub-parallel to the topographic surface. They initially form through a combination of the ambient stress field and stress perturbations caused by topographic loading and fluid pressure. For recent, more detailed studies of the initiation, propagation and development of sheeting joints see Martel (2017) and Moon et al. (2017). Today, the sub-Cambrian peneplain, fragmented by the block movements and modified by Quaternary glacial erosion and described in this report, is widely exposed subaerially and in most of the submarine portion of the study area (Figure 2-4).

Although seismic activity occurs within and close to the study area ([www.snsn.se](http://www.snsn.se)), no conclusive evidence has been found for formation of the fault scarps exclusively through post-glacial earthquakes (Lagerbäck et al. 2005). In a more recent LiDAR-based geomorphological study of the area, Öhrling et al. (2018) report cross-cutting relationships between glacial morphological features and two fault scarps that could potentially be the result of post-glacial faulting. However, to assess the timing of the faulting Öhrling et al. (2018) suggest that the identified fault scarps be further examined through field work.



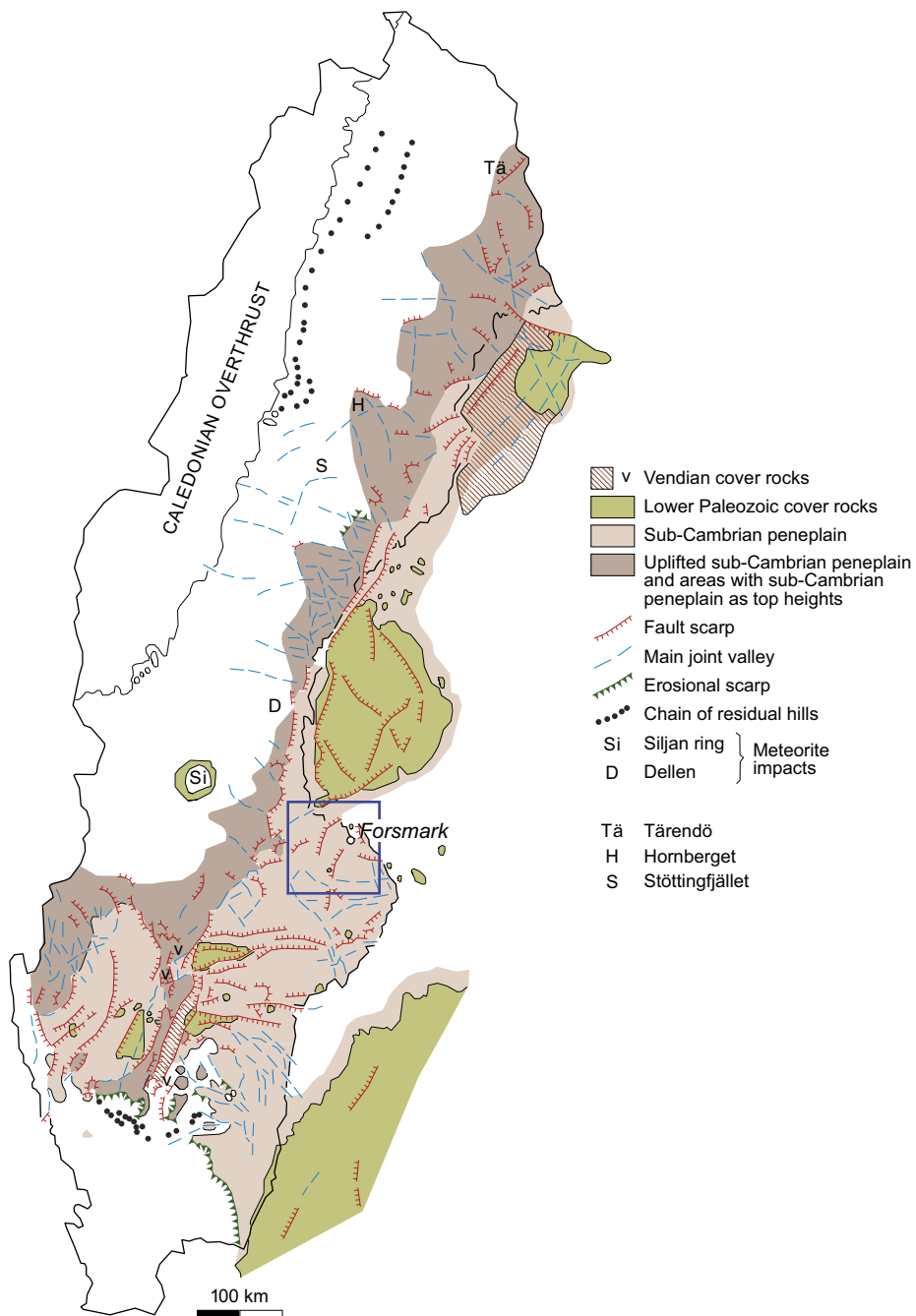


**Figure 2-4.** Inferred extent of the sub-Cambrian peneplain and location of the study area. Figure from Lidmar-Bergström and Olvmo (2015).



### 3 Methodology

Figure 3-1 summarises the workflow applied to produce a rock block model. The individual steps are detailed in the succeeding sections. First, digital elevation data and bathymetric data need to be combined to a common DEM, which is then gridded to  $50 \times 50$  m resolution. Based on the DEM, lineaments are interpreted from topographic lows and are used to define the block boundaries. Second, the bedrock elevation model is produced by subtracting the overburden thickness from the DEM. The resulting bedrock elevation model corresponds approximately to the faulted and glacially eroded sub-Cambrian peneplain. The topographic gradient is then removed from the bedrock elevation model and maximum elevation values calculated for each rock block. The method builds entirely on the assumption that the original relative relief of the sub-Cambrian peneplain was less than 20 meters in the study area (Rudberg 1960, Olvmo 2010).

#### 3.1 Base data

Since the study area extends across both land and sea, digital elevation and bathymetric data need to be combined to a common DEM. The on-shore elevation data is based on the national elevation model (Nationella Höjdmodellen “NH”) produced by the Swedish land survey (Lantmäteriet) from LiDAR measurements and which has a horizontal grid resolution of  $2 \times 2$  m. Bathymetric contour lines from the Swedish Maritime Administration (Sjöfartsverket) were used to interpolate a sea floor surface using a combination of the Topo-to-Raster and Aggregate functions in ArcMap™ (version 10.5.1, ESRI 2017) with a final horizontal resolution of  $50 \times 50$  m. This resolution was chosen in order to bridge the difference between the high-resolution terrestrial elevation and the contour-based bathymetric data. Due to the choice of resolution, any structures that are smaller than 50 m cannot be resolved. The resulting combined DEM is presented in Figure 3-2.

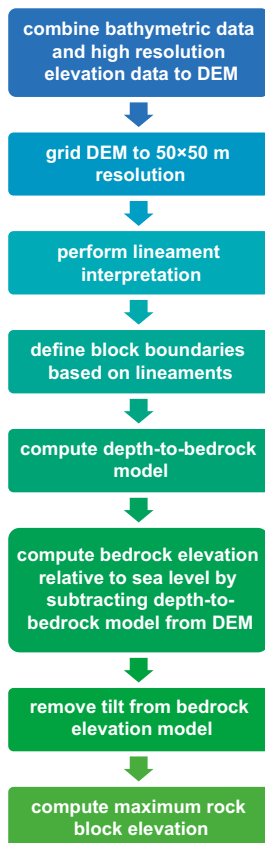


*Figure 3-1. Flow chart illustrating the various steps necessary to compute the maximum values for the rock block elevation.*

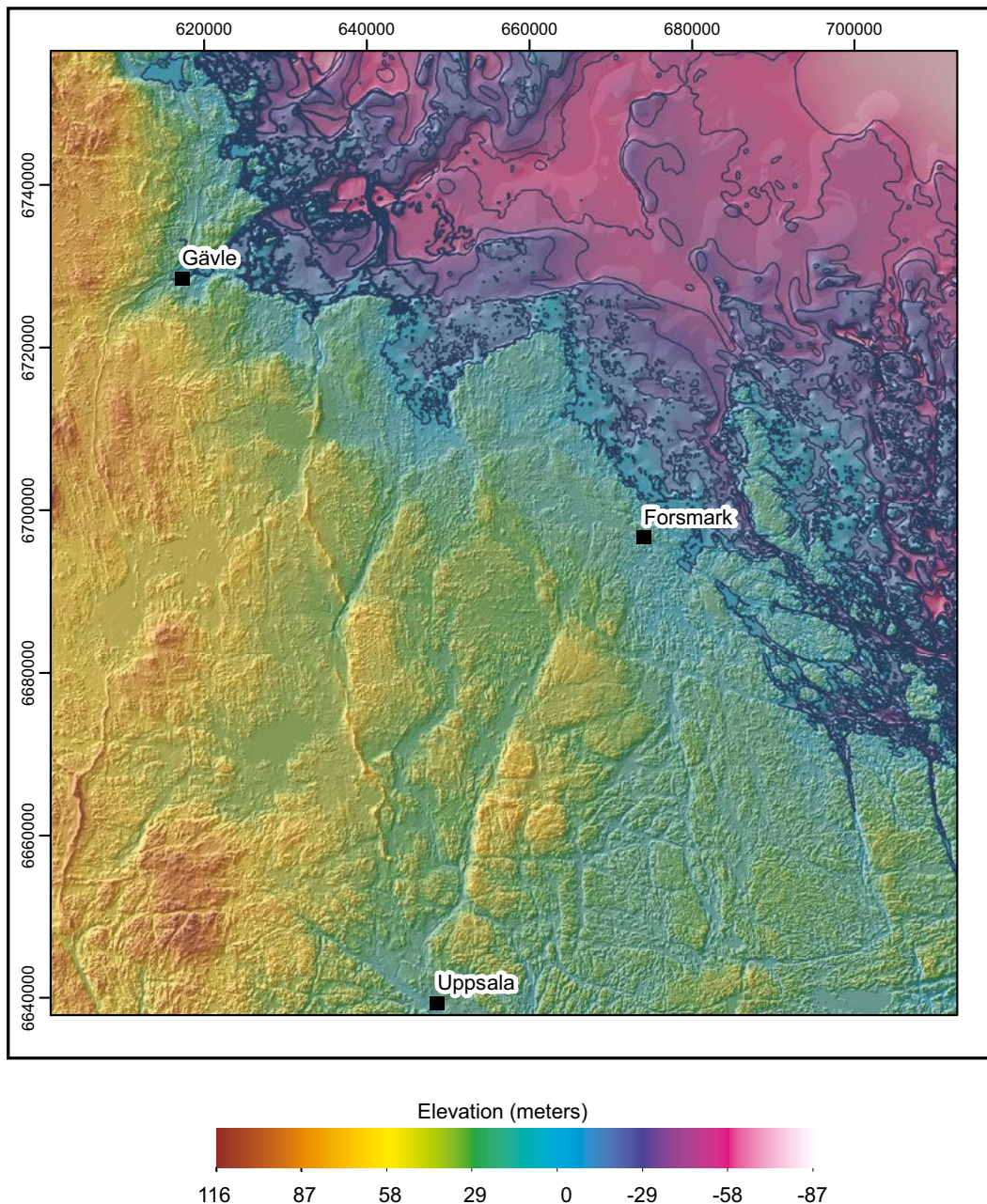
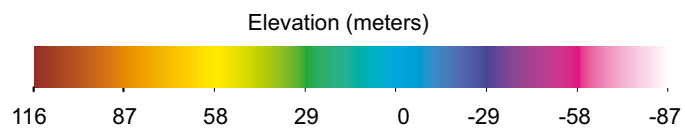
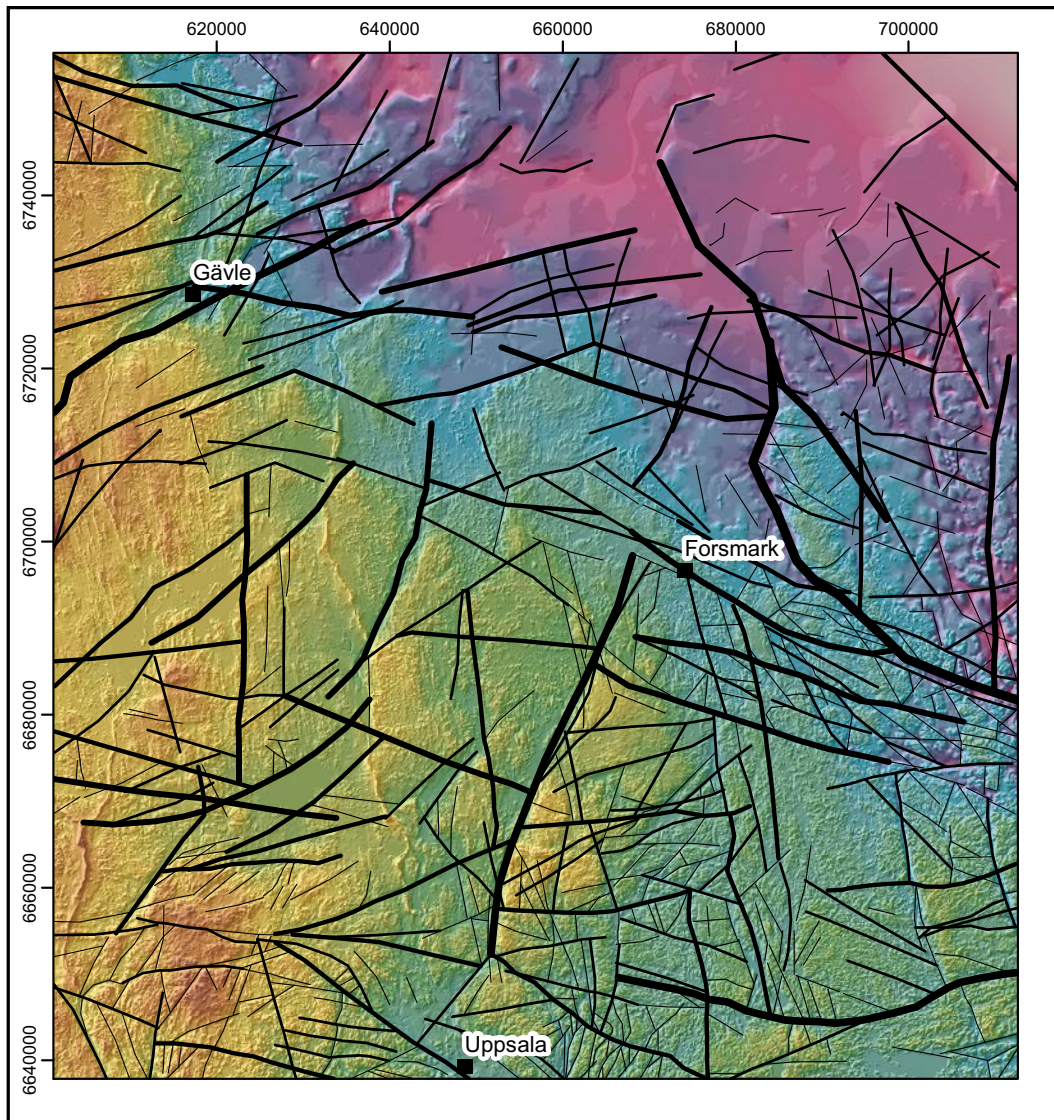


**Figure 3-2.** Combined digital elevation model (DEM) produced by merging the National Elevation Model (Lantmäteriet) and the sea floor bathymetry model. The DEM represents the relief of both the bedrock surface and the Quaternary cover sediments. This DEM is the base model used for all later calculations. The blue contour lines were used for the interpolation of the bathymetric data. Coordinates are in meters (SWEREF99TM).

### 3.2 Lineament interpretation and rock block boundaries

Bedrock that has been affected by deformation through brittle faulting or fracturing is more easily eroded than intact bedrock. Continuous, nearly straight topographic minima observed in a DEM, i.e. lineaments, are therefore generally thought to reflect brittle structures in the bedrock. Lineaments were interpreted based on such topographic minima in the combined DEM (Figure 3-3). For the lineament interpretation the scale was “locked” to 1:250000 in ArcMap™ (version 10.5.1, ESRI 2017). At that scale, the shortest lineament that was identified was approximately 1 200 m long.





Topographic lineaments

- < 10 km
- 10-20 km
- 20-30 km
- 30-40 km
- 40-50 km
- 50-60 km

**Figure 3-3.** Topographic lineament interpretation of the combined digital elevation model. Black lines are lineaments interpreted based on the DEM with 50 m grid resolution. The DEM represents the relief of both the bedrock surface and the Quaternary cover sediments. The lineament line thickness indicates different length categories. The coordinate values are in meters (SWEREF99TM).



Off-shore reflection-seismological profiles (Nyberg and Bergman 2012, Nyberg 2016) were also used to interpret potential faults, and the topographic lineaments were adjusted accordingly. Additionally, a higher resolution bathymetric map (SGU) was used to correct the position of the lineaments. However, these newer bathymetric data are classified and are therefore not included in the present report nor in the deliverables to SKB's databases.

The lineament maps provide the base for defining the rock block boundaries (Figure 3-4). In some places, the length of the lineaments was extended to form closed polygons. Such an extension was only performed if it was less than 10 to 20 % of the total lineament length. Additionally, if a lineament ceased inside a neighbouring rock block polygon and did not cross it more than 50 % along its main direction, the section of the lineament inside the polygon was erased.

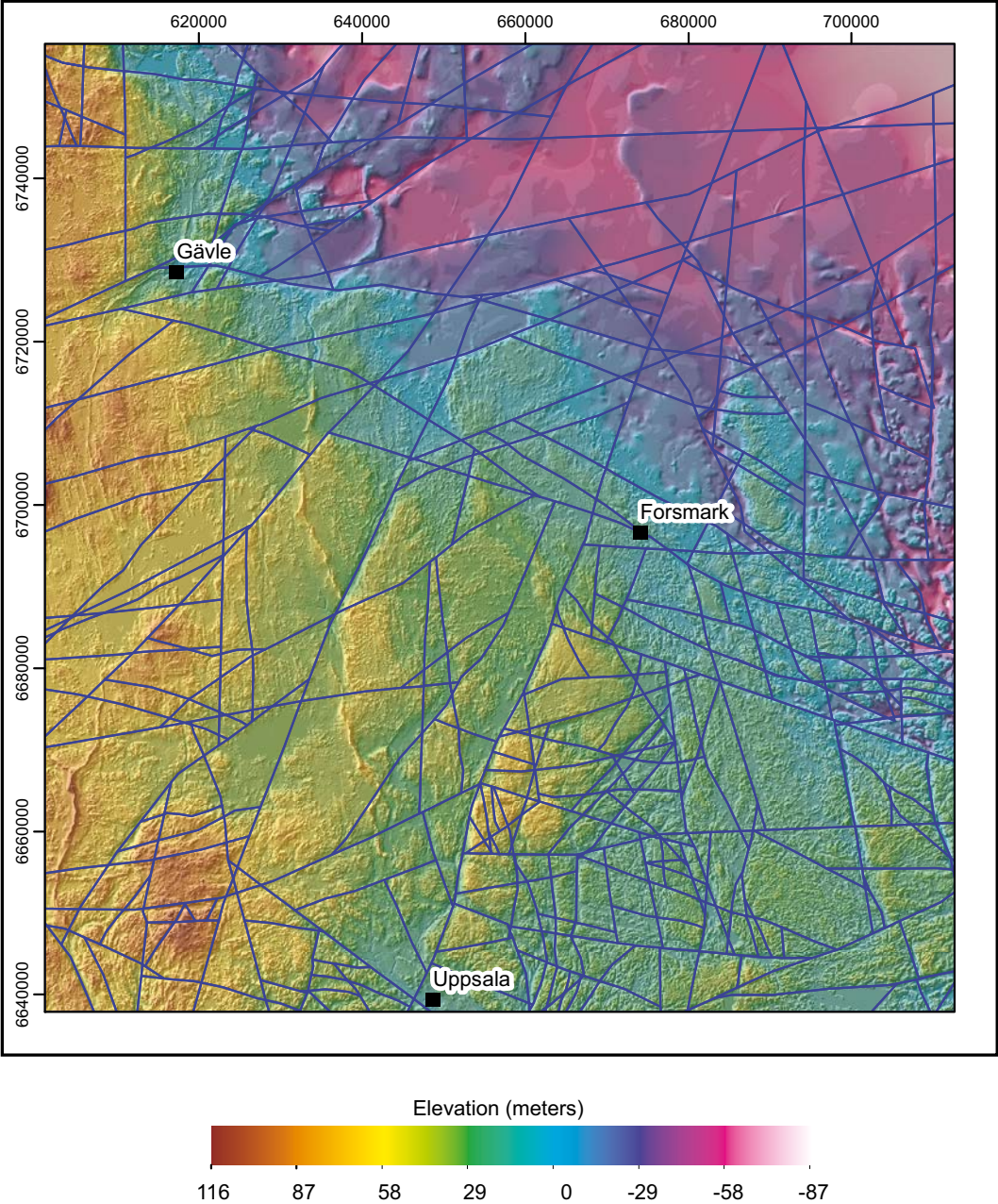


**Figure 3-4.** Rock block model (blue lines) for the study area. Background map is the combined DEM. The DEM represents the relief of both the bedrock surface and the Quaternary cover sediments. Coordinates are in meters (SWEREF99TM).

### 3.3 Depth to bedrock and bedrock elevation relative to sea level

An algorithm developed in-house at SGU was used to produce a model for the depth to bedrock and the bedrock elevation relative to sea level (Figures 3-5 and 3-6). The depth-to-bedrock model (Figure 3-5) is based on point data with information on overburden thickness, i.e. the thickness of the Quaternary sediments covering the bedrock. The combined DEM of the land surface and the seafloor is used to calculate the bedrock elevation model (cf. Figure 3-3).

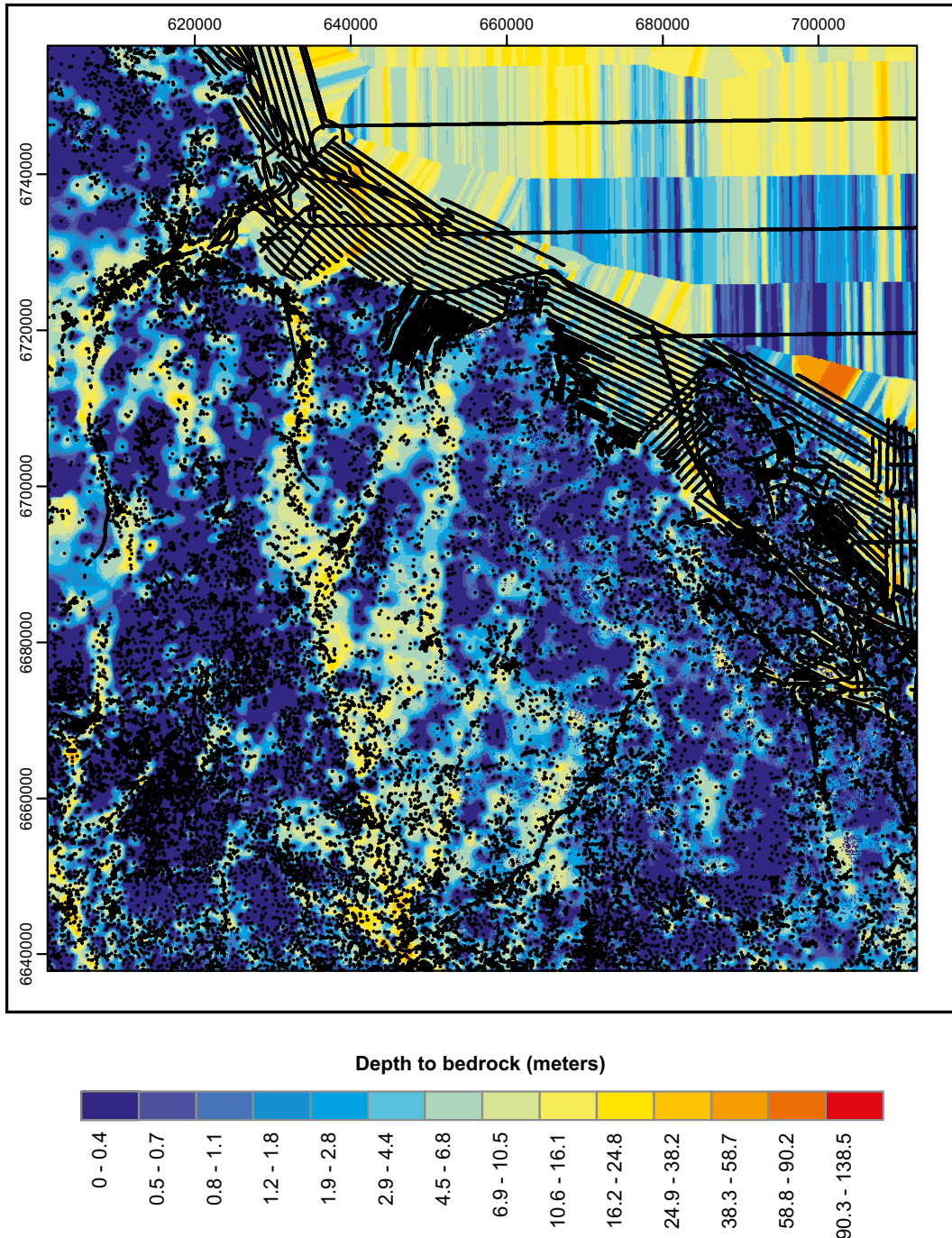


*Figure 3-5. Model showing depth to bedrock, i.e. the thickness of the Quaternary sediments in the study area. Black dots show distribution of point data with depth information. Coordinates are in meters (SWEREF99TM).*



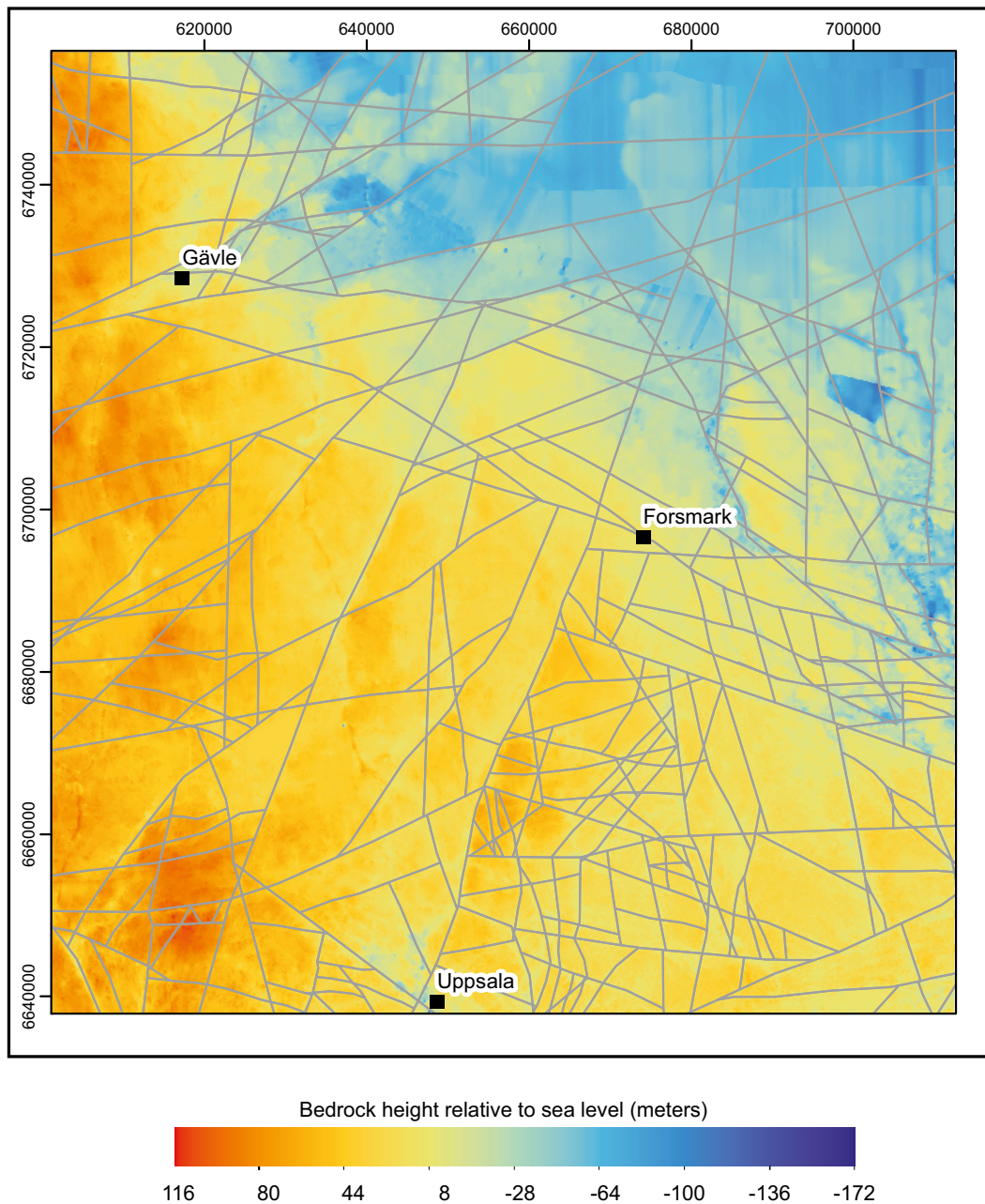


**Figure 3-6.** Model for bedrock height relative to sea level. Coordinates are in meters (SWEREF99TM).

Overburden thickness point data were combined from multiple sources:

- Quaternary deposits within the SGU Quaternary deposits map as well as data collected by SGU from other sources, such as geotechnical consultants and the Swedish Transport Administration (Vägverket) (n = 9 251).
- SGU well database (n = 27 128).
- petrography and seismic SGU databases (n = 1 429).
- interpreted marine geophysical profiles (n = 72 837) that are the base to the marine geological maps Eggegrund-Gävle (Nyberg and Bergman 2012) and Södra Bottenhavet (Nyberg 2016).

A total of ca. 120 000 data points were used as input into the block model (Figure 3-5). Despite their high number, the points are not evenly distributed across the area. This is particularly apparent in the off-shore part of the study area where the data points are derived from geophysical survey lines. Even if data points along some lines are closely spaced (as low as 10 meters) in some locations, the spacing between the lines is much higher. For example, the line spacing is up to 13 km in the north-eastern part of the study area, but only ca. 800 m in the Gävle area (Nyberg and Bergman 2012, Nyberg 2016, see also Figure 3-5). Consequently, artefacts can occur when interpolating the data points to surfaces and are the reason for the anonymously low topography to the east of Gräsö (Figures 3-5 and 3-6).

The depth to bedrock was modelled as a surface interpolated from all available depth data points from the Inverse Distance Weighted (IDW) method included in ArcMap™ (version 10.5.1, ESRI 2017). IDW uses a linearly weighted combination of a set of data points to interpolate the surface (Philip and Watson, 1982). The amount of selected points is based on the ‘exponent of distance’, here set to the default value “2” due to the uneven distribution of depth data points. The cell size of the output raster is 50 meters.

Bedrock elevation relative to sea level is modelled by subtracting the depth-to-bedrock model from the land and seafloor surface. The morphology of the resulting bedrock elevation model (Figure 3-6) reflects approximately the present shape of the tectonically dislocated and glacially eroded sub-Cambrian peneplain. Quaternary glacial erosion has lowered the existing bedrock surface from the original unconformity and has also varied spatially in its magnitude (Hall et al. 2018). Palaeozoic sedimentary rocks are also included in the bedrock elevation model along the northern margin of the study area. Bedrock elevation ranges from -172 m under water to +116 m on land. It is to be noted that the extremely low submarine values may be an artefact from the interpolation and may also reflect the quality of the data used to produce the depth-to-bedrock model. An artefact is obvious in a small triangular area in the north-eastern part of the study area. Overall, there is a gradient in bedrock elevation from high values in the west and southwest to low values in the northeast of the study area (Figure 3-6).

### 3.4 Correction for topographic gradient

The present bedrock surface displays a regional dip towards the NE with a topographic gradient of ca. 0.01 %. To focus on relative block movements, this regional topographic gradient is removed by subtracting a trend surface from the bedrock elevation model. The trend surface is calculated in ArcMap™ (version 10.5.1, ESRI 2017) by dividing the study area into a grid of 2×2 km sized squares and extracting maximum bedrock elevation points for each square from the model for bedrock height relative to sea level. Those points are closest in elevation to the former “uneroded” sub-Cambrian peneplain and are also likely to have the least glacial erosion because generally they will be in rock compartments with low vertical fracture frequency. The Global Polynomial Interpolation tool in the Geostatistical Analyst Toolbox (ArcMap™ (version 10.5.1, ESRI 2017)) is then used to fit a trend surface through these maximum elevation points. In this study, solutions for trend surfaces of 1<sup>st</sup>, 2<sup>nd</sup>, and 3<sup>rd</sup> degree polynomials (Figure 3-7) are presented. The higher the polynomial degree, the higher the root mean square value, i.e. the closer the trend surface becomes to the “true” shape of the dislocated sub-Cambrian peneplain. The resulting back-tilted bedrock elevation models for the three different polynomials are presented in Figure 3-7 (“Poly1”, “Poly2”, “Poly3”). The resulting models differ most for lower degree polynomials whereas differences between models of higher degree polynomials wane. The linear trend surface (“Poly1”) is arguably the preferred surface to use to correct for the regional topographic gradient because it will provide a surface that is intermediate in elevation between the raised and lowered fault blocks.

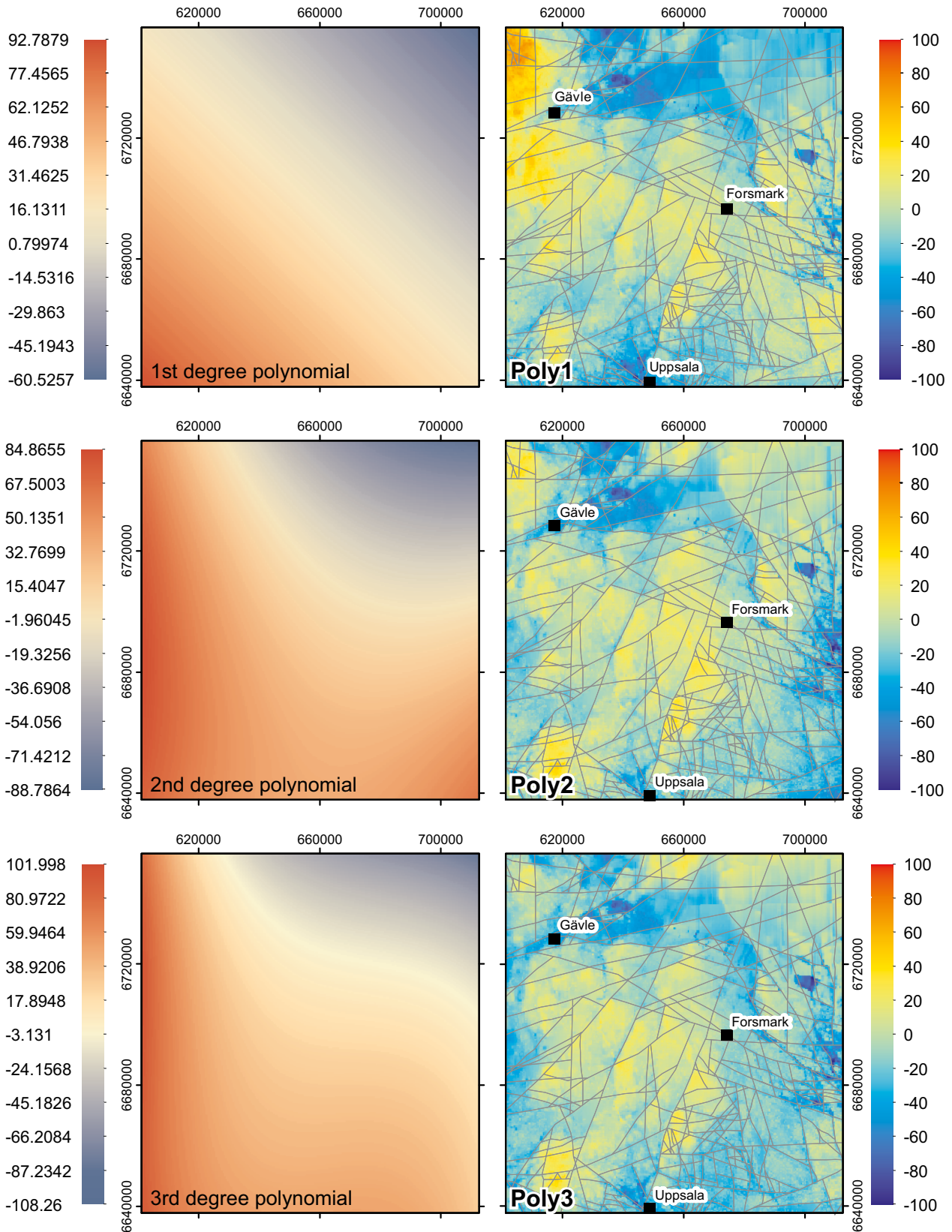


**Figure 3-7.** Polynomial trend surfaces (left column) and resulting models for bedrock elevation relative to sea level (right column) after subtraction of trend surfaces. As polynomials increase, the trend surface approaches the “real” shape of the bedrock surface. Compare to original bedrock elevation model in Figure 3-5. Note that the elevation values in the left column have the same colour scale but different minimum and maximum elevation values. Coordinates are in meters (SWEREF99TM).



## 4 Results

### 4.1 Maximum rock block elevation

Based on the corrected bedrock elevation models (Figure 3-7), the maximum bedrock elevation was calculated for each rock block using the Zonal-Statistics-as-Table tool in ArcMap™ (version 10.5.1, ESRI 2017). Table 4-1 lists the key statistics for all three models.

**Table 4-1. Maximum rock block elevation for different bedrock elevation models after removal of the topographic gradient. All values are in meters. “Relative difference” is the relative height difference between the minimum and maximum height values for the respective models.**

Model	Maximum bedrock elevation (m)		
	Lowest block elevation	Highest block elevation	Relative difference
Poly1	-51.9	81.4	133.3
Poly2	-55.5	51.7	107.2
Poly3	-41.4	48.5	89.9

Figure 4-1 visualises the maximum rock block elevation for the three different bedrock elevation models (Poly1, Poly2, Poly3), and Figure 4-2a–c shows histogram plots visualising the frequency distribution of the maximum rock block elevation for the three different models.

Regardless of the polynomial degree chosen for the correction of the bedrock elevation model, the resulting block models for the maximum elevation (Figure 4-1) show that the elevation of the bedrock surface is uneven between blocks, resulting in some blocks being located higher than the mean regional bedrock summit elevation and some being located lower (Figure 4-1). All three models show positive maximum bedrock elevation values for blocks in the central part of the study area (Figure 4-1). Blocks with positive maximum elevation values also occur in the south-west and north-west parts of the study area. In model Poly1, the blocks with the highest elevation occur west of Gävle in the northwest corner of the study area. Blocks with negative maximum elevation values occur predominantly in the south and south-east of the study area as well as in the north-north-west along the Gävle graben. There may be three reasons for that: less relative fault movement, more glacial erosion (around Uppsala) and more glacial erosion of Jotnian and early Paleozoic cover rocks, e.g. in the Gävle graben. The relative difference in bedrock elevation between the block with the highest maximum elevation and the block with the lowest maximum elevation lies between ca. 90 and 133 m for all models (Table 4-1, “Relative difference”).

The histograms for the maximum rock block elevation show a bell-shaped frequency distribution for all models (Figure 4-2a–c). The peak of the bell-shaped distribution for the maximum elevation lies between ca. +20 and -20 m (Figure 4-2a–c). This indicates that, on average, most of the rock blocks have not been displaced very much at all, which is also reflected by the large number of greenish-coloured blocks in Figure 4-1.

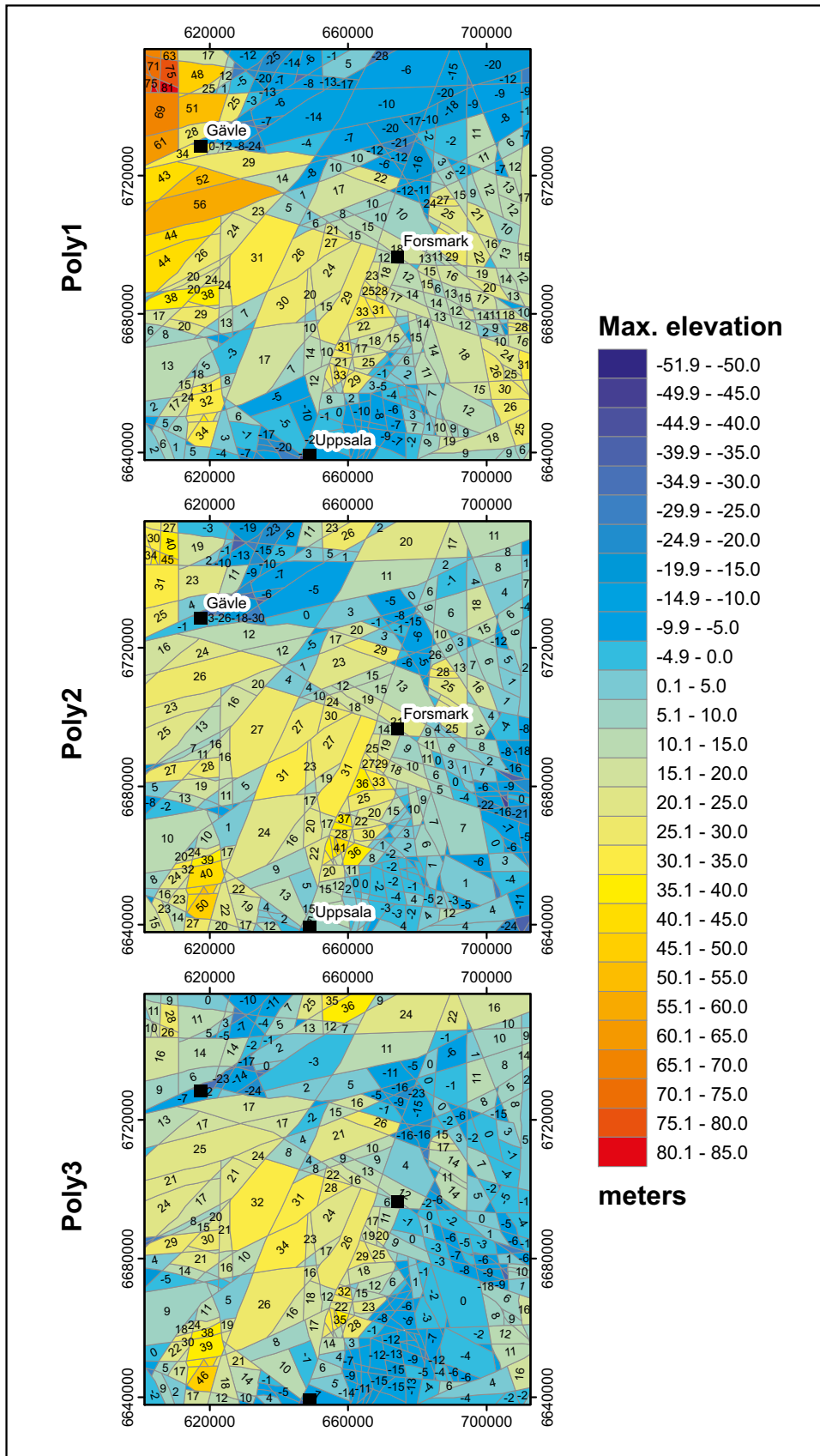


**Figure 4-1.** Maximum rock block elevation for different bedrock elevation models after removal of the respective topographic gradient. From top to bottom Poly1, Poly2, Poly3. The number labels indicate the maximum elevation of the individual blocks.

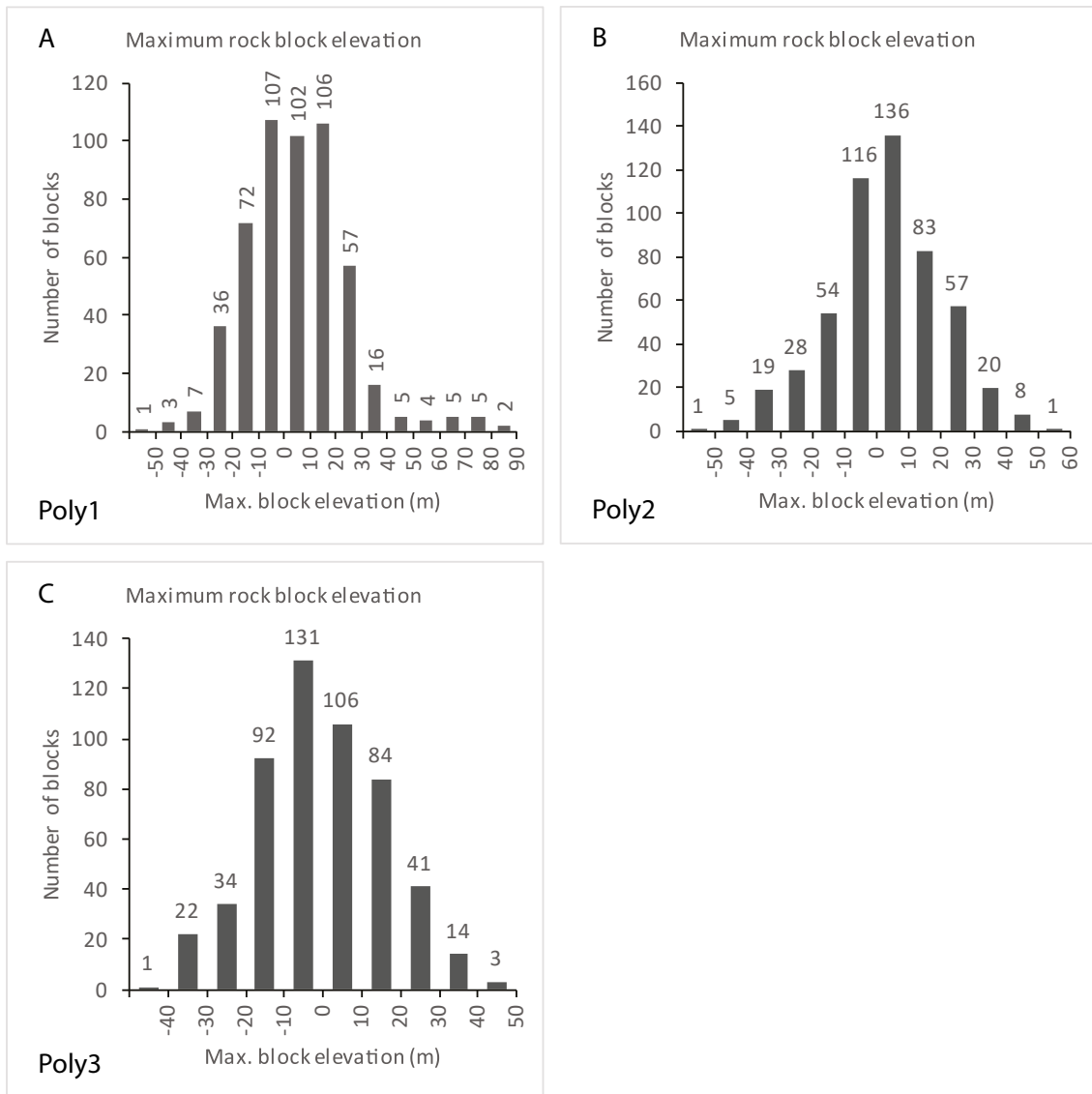


**Figure 4-2.** Maximum rock block elevation frequency distribution for model (A) Poly1, (B) Poly2, (C) Poly3. Note the bell-shaped distribution of the elevation values.



## 5 Discussion

### 5.1 Interpolation of trend surface for removal of topographic gradient

The polynomial trend surface that is subtracted from the original bedrock elevation model (cf. Figure 3-7) depends on the distribution of the maximum bedrock elevation points in the original model which in turn depends on the mesh size of the grid. Grids with larger mesh size (4×4 km and 10×10 km) were tested, but differences in the resulting trend surfaces are negligible. For the purpose of this study, the choice of a grid with a 2×2 km quadratic mesh is considered reasonable.

The factor controlling the shape of the un-tilted bedrock elevation model, and consequently the maximum elevation values for each single block, is the polynomial degree chosen of the trend surface for the removal of the topographic gradient from the original bedrock elevation model. The most apparent difference between the resulting back-tilted bedrock elevation models occurs in the northwest corner of the study area, where model Poly1 shows a considerably higher bedrock elevation than models Poly2 and Poly3 (cf. Figure 3-7). However, for the rest of the area, bedrock elevation lies roughly in the same range for all three models (cf. Figure 3-7). Still, the polynomial degree is of minor importance for this study because the relative differences in rock block elevation may vary by some meters and no polynomial can erase or invert these relationships. Blocks that have moved upward have a higher bedrock elevation than their neighbouring blocks and vice versa, even for higher order polynomials.

### 5.2 Relative block movement

The unequal elevation of the bedrock surface across the study area implies that the sub-Cambrian peneplain and its Palaeozoic cover rock remnants have been displaced vertically by relative block movements during the Phanerozoic, prior to glacial erosion. The relative block displacement between adjacent blocks can exceed 20 m (Figure 4-1). All vertical displacement values are net apparent displacements since it is unclear to what extent and under what stress regimes faults have been reactivated. Also, for the rock block models it is assumed that the individual blocks moved uniformly, i.e. the models do not account for potential rock block tilting or rotation. The bedrock elevation models in Figure 3-7 clearly show, though, that the bedrock surface is tilted within some of the blocks.

The most apparent rock block movement occurred along NNE-SSW and NNW-SSE striking block boundaries that run parallel to old brittle-ductile shear zones such as the Österbybruk-Skyttorp and the Gimo deformation zone (cf. Figures 2-2 and 4-1). In the Gävle graben area, blocks have been down-faulted along graben-parallel faults striking WSW-ENE (e.g. Figure 4-1). Some minor block movement is also inferred across block boundaries running parallel to the WNW-ESE striking Singö shear zone system.

To illustrate the displacement and locally tilting of the peneplain, five profile lines are drawn across the corrected bedrock elevation using model Poly1 as an example (Figure 5-1). The bedrock elevation models are shown in Figure 5-2a–c and roughly illustrate the stepped offset of the sub-Cambrian peneplain and its younger sedimentary cover rocks.

Sub-parallel profiles A-B, A'-B' and A''-B'' indicate east-side up fault movement and eastward-tilting of blocks on NNE-SSW striking faults (Figure 5-2a). Since the dip of these faults is not known, they are here indicated as vertically dipping and with normal dip slip movement. However, since in the past, and at present, the maximum horizontal stress is oriented NW-SE at least in the upper ca. 1 000 m (e.g. Martin 2007 and Figure 2-1), the possibility cannot be excluded that these faults may be east-dipping and may have been reactivated in a reverse sense.

Profile C-K-D (Figure 5-2b) extends sub-parallel to the Österbybruk-Skyttorp deformation zone and crosses the Forsmark and Singö deformation zones. In the southwestern part of profile C-K-D the sub-Cambrian peneplain is tilted towards the south whereas towards the northeastern part, the surface is tilted towards the north. It also seems that the bedrock surface has been uplifted and down-faulted along more or less ENE-WSW striking faults in the central part and along WNW-ESE striking faults parallel to the Forsmark and Singö deformation zones (cf. Figure 5-1). Alternatively, glacial erosion of the summits parallel to the ÖSZ may have caused a depression in the elevation profile. The block between the Forsmark and Singö deformation zones is uplifted if only by a few meters (Figure 5-2b), which is in agreement with the observations by Söderbäck (2008).

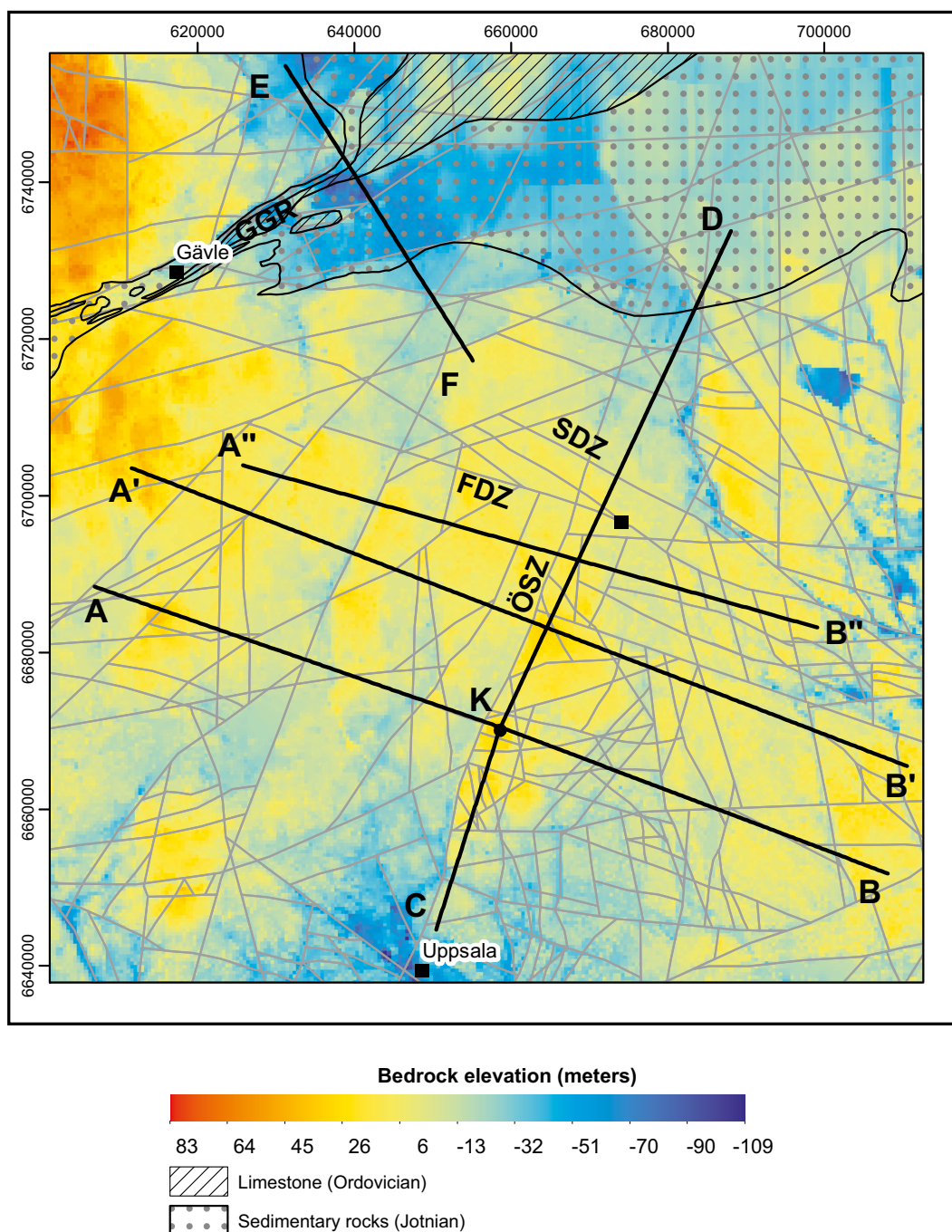


**Figure 5-1.** “Corrected” Bedrock elevation model Poly1 with location of elevation profiles A-B, A'-B', A''-B'', C-K-D and E-F in Figure 5-2a-c. ÖSZ: Österbybruk-Skyttorp deformation zone, FDZ: Forsmark deformation zone, SDZ: Singö deformation zone, GGR: Gävle graben.

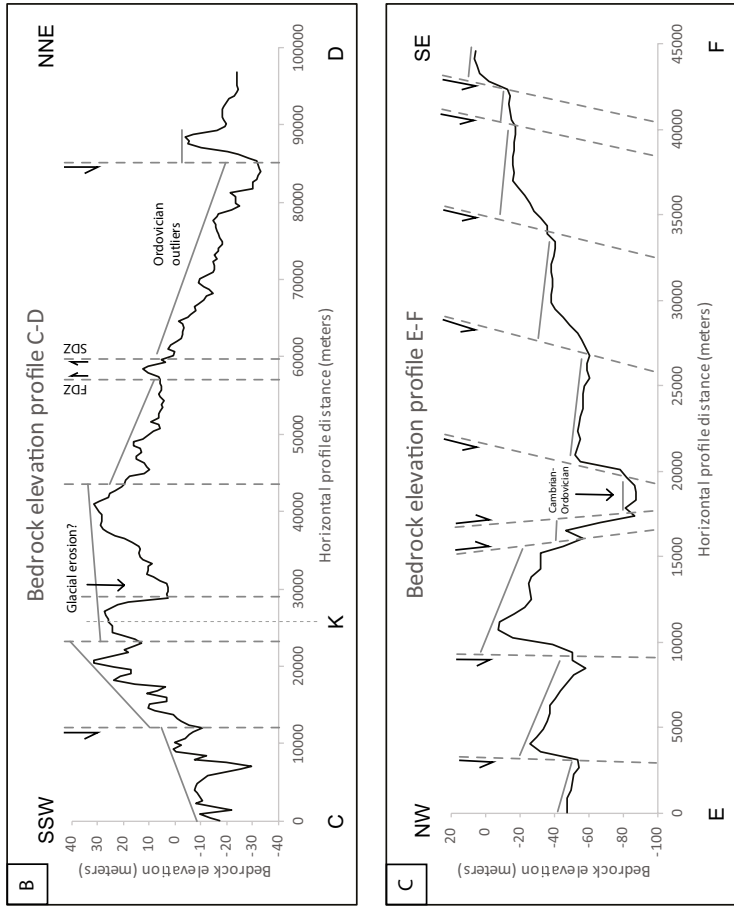
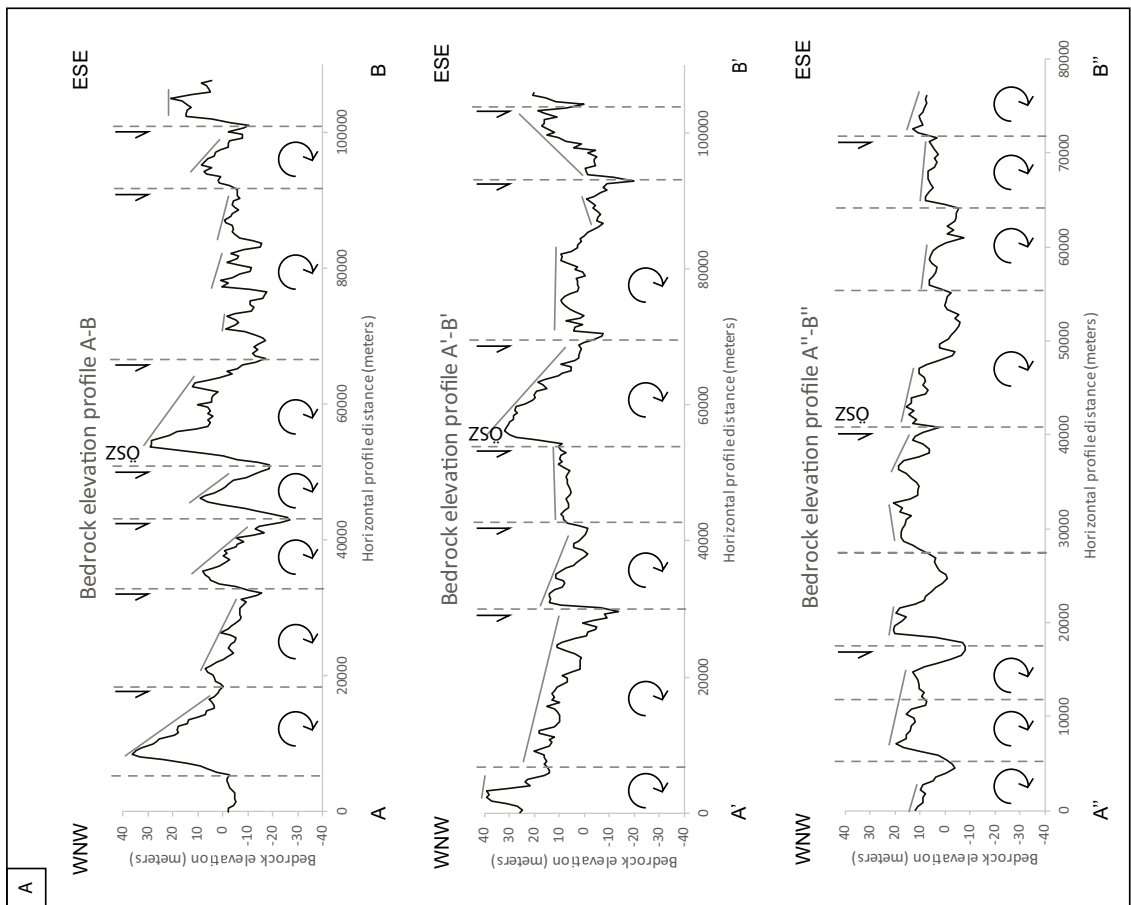


**Figure 5-2.** Bedrock elevation profiles across model Poly1 and conceptual fault models. Location of profiles indicated in Figure 5-1. ÖSZ: Österbybruk-Skyttorp deformation zone, FDZ: Forsmark deformation zone, SDZ: Singö deformation zone. (a) Profiles A-B, A'-B', A''-B''. Faults are here indicated with normal movement. The faults may, however, dip to the ESE and in that case would have accommodated reverse movement. (b) Profile C-K-D, (c) Profile E-F. The bedrock surface in profile E-F appears comparably smooth due to low spatial resolution of the elevation data. Note that the straight grey lines are merely added as a visual aid and only very roughly approximate the bedrock surface.

Profile E-F crosses the ENE-WSW striking Gävle graben (Figures 5-1 and 5-2c). The graben structure is clearly visible in that the peneplain has been displaced and tilted by normal faulting. The cumulative slip is ca. 80 m in the central part of the profile. This is a minimum estimate, since even here, the current NW-SE directed maximum horizontal stress would lead to graben inversion and therefore reactivation of the normal faults as reverse faults. Some of the graben faults must have been active during and after the Ordovician since there are Ordovician limestones that are bounded by these faults (cf. Bergman et al. 2005 and Figure 5-1). Quaternary glacial erosion may not have contributed to much of the development of the topographic low in the Gävle graben because it is oriented transverse to the direction of ice flow (Hall et al., submitted). It may, however, have eroded rock from the higher lying graben shoulders, hence decreasing the apparent offset.

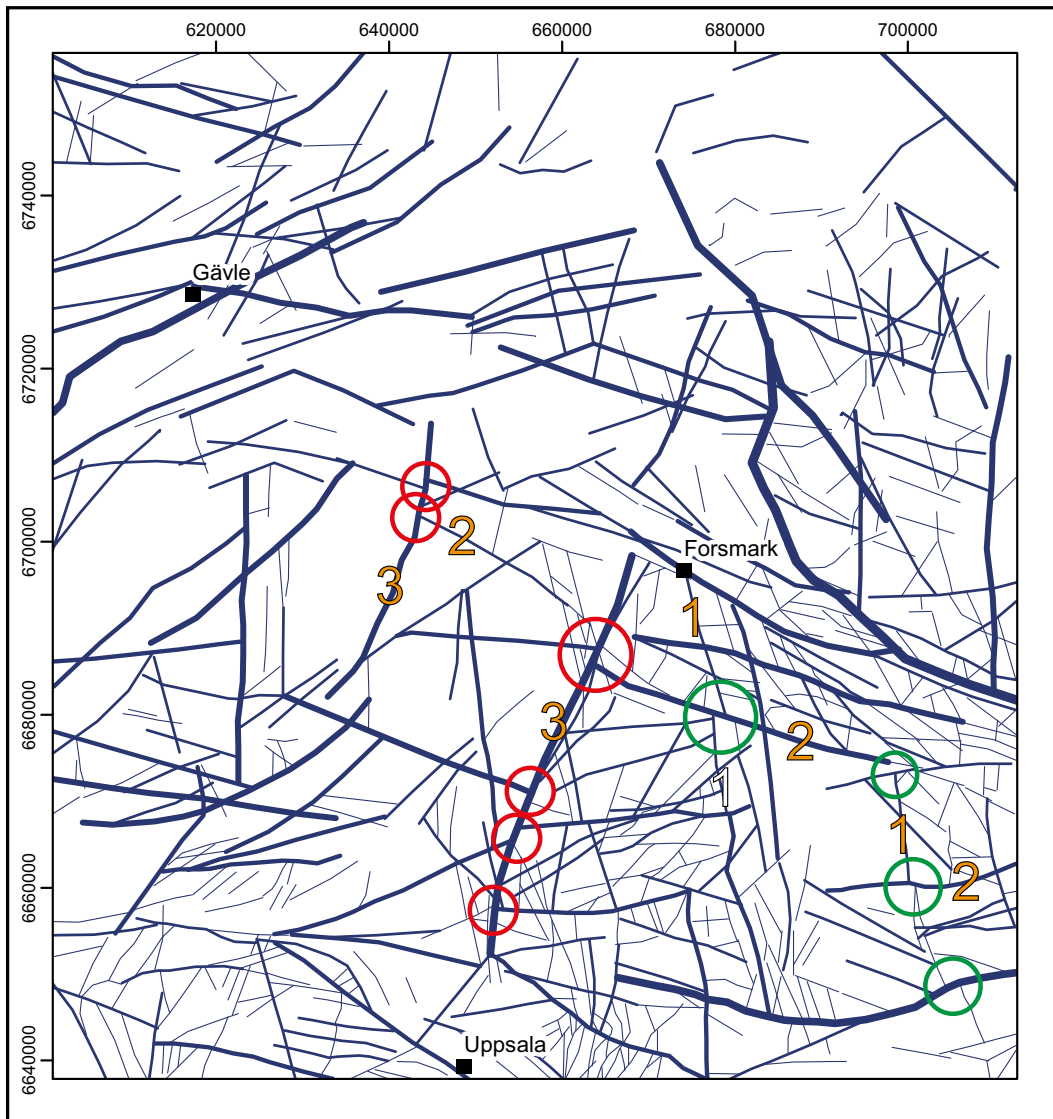
### **5.3 Relative fault timing based on lineament abutting relationships**

Some seemingly systematic abutting relationships between lineaments of different orientations are marked in Figure 5-3. NNW-SSE to N-S-striking lineaments locally abut against WSW-ENE and WNW-ESE-striking lineaments (green circles in Figure 5-3). In turn, some of the WNW-ESE and WSW-ENE trending lineaments abut against NNE-SSW striking lineaments (red circles in Figure 5-3). However, great care must be taken when attempting to interpret these relationships in terms of relative fault timing. The general hypothesis that younger fractures abut against older ones only holds if the older fracture has aperture or is filled with very weak gouge acting like a weak fluid, and if the opening mode of the younger fracture is purely extensional since that type of fracture cannot propagate across a free surface (Twiss and Moores 2007, chapter 2.4). Also, secondary structures such as Riedel shears often form synchronously to a shear fracture but appear as though they were abutting against the main fracture. In the study area, a further complication is the fact that most of the deformation zones have been reactivated, some of them multiple times under variable stress conditions (e.g. Sandström et al. 2009, Saintot et al. 2011). Hence, what seems like abutting relationships on the lineament map probably reflects displacement of older deformation zones along the cutting structure. Highly speculatively, this may indicate a faulting sequence post-dating the formation of the Sub-Cambrian peneplain as follows: (1) NNW-SSE-striking structures which are displaced by (2) WSW-ENE- and WNW-ESE-striking zones which in turn are faulted by (3) NNE-SSW to NE-SW striking deformation zones (Figure 5-3). Saintot et al. (2011) report the possibility of Permo-Carboniferous rifting in the Forsmark area, and the Permian adularia age derived from a NE-SW oriented fracture (Sandström et al. 2006, 2009) may indicate a NW-SE extensional stress field which could correspond to the hypothetically youngest reactivation (see above). This is supported by recently observed slickensides indicating normal faulting on a steeply WNW-dipping fault within the Österbybruk-Skyttorp deformation zone (S. Luth, personal communication). However, without any further field reconnaissance it is difficult to verify the proposed faulting sequence.

### **5.4 Rock block model limitations**

The rock block models only approximate the results of the tectonic dislocation of the sub-Cambrian peneplain because there are some uncertainties to be considered. Firstly, the models do not account for the fault mechanisms that caused the faulting because all displacements measured on block boundaries or faults are assumed to have occurred on vertical fault planes and do not account for dip angles other than 90°. This also implies that block movement occurred strictly by dip slip and no strike slip or rotational movement is considered.





Topographic lineaments 1:250000

- < 10 km
- 10-20 km
- 20-30 km
- 30-40 km
- 40-50 km
- 50-60 km

**Figure 5-3.** Lineament map (cf. Figure 3-3). Highly speculative interpretation of abutting relationships between lineaments may indicate that NNW-SSE-striking structures (1) may be displaced by (2) WNW-ESE- and WSW-ESE-striking structures (green circles), which in turn may have been displaced by (3) NNE-SSW-striking structures (red circles). Coordinates are in meters (SWEREF99TM).

Further, considering the net vertical displacement of the bedrock blocks, the models do not differentiate between vertical displacement along a steep fault and vertical displacement by shallowly dipping structures such as sheet joints. Also, the models show the state of the bedrock surface as-is, which means that, without further geological investigations, fault inversion remains undetected. This implies that all displacement values are apparent and should be interpreted as minimum values on faults that may have been reactivated as reverse faults in past regional stress fields or in the current one.

Another uncertainty is the amount of erosion by ice during the Quaternary period. For example, Hall et al. (2018) suggest glacial erosion of 2–3 meters at bedrock summits during the latest glaciation based on surface exposure dating using terrestrial cosmogenic nuclides. Averaged over 1 million years, Hall et al. (2018) model erosion rates of 20–40 m/Myr, depending on the type of erosion. They assume slow erosion rates for continuous abrasion and fast erosion rates for episodic abrasion in combination with plucking (Hall et al. 2018). Because these inferences are for summits, these must be minimum values for this landscape. This also supports the assumption that the block displacements are minimum values. Higher magnitude glacial erosion occurred in fracture and deformation zones that strike NW-SE because of the coincidence with ice flow direction (Hall et al., submitted). Glacial erosion may therefore have contributed to deepening in locations such as to the east of Gräsö, where the bedrock elevation models indicate exceptional low elevation for this landscape (cf. Figure 3-6).

## 6 Conclusions

Rock block models provide a tool for detecting and characterising Phanerozoic fault movement using the sub-Cambrian peneplain as a reference surface. The newly calculated rock block models in this study show that Phanerozoic dip slip movement dominantly occurred along WNW-ENE and NNE-SSW striking faults. Assuming that glacial erosion can be neglected, the offset across these faults is of the order of tens of meters. Normal faulting across ENE-WSW striking faults has affected the bedrock surface in the Gävle graben, where dip slip is locally more than 20 meters across a single normal fault and cumulative slip adds up to around 80 meters.



## **Acknowledgements**

We thank Raymond Munier, Jens-Ove Näslund and Bradley Goodfellow for fruitful discussions and their comments on an early version of the manuscript. Constructive and detailed reviews by Adrian Hall and Diego Mas Ivars were highly appreciated and contributed greatly to enhance the quality of this report.



## References

SKB's (Svensk Kärnbränslehantering AB) publications can be found at [www.skb.com/publications](http://www.skb.com/publications).

**Ahl M, Andersson U B, Lundqvist T, Sundblad K (eds), 1997.** Rapakivi granites and related rocks in central Sweden : 7th International Symposium on Rapakivi Granites July 24–26 1996, University of Helsinki, Finland : excursion July 16–23 1996. Uppsala: Geological Survey of Sweden. (SGU series Ca 87)

**Ahlberg P, 1986.** Den svenska kontinentalsockelns berggrund: sammanfattning av tillgängliga undersökningar. Uppsala: Sveriges geologiska undersökning. (Rapporter och meddelanden 47) (In Swedish.)

**Amantov A, Laitakari I, Poroshin Y, 1996.** Jotnian and Postjotnian: Sandstones and diabases in the surroundings of the Gulf of Finland. Geological Survey of Finland, Special Paper 21, 99–113.

**Beckholmen M, Tirén S A, 2010a.** Rock-block characterization on regional to local scales for two SKB sites in Forsmark – Uppland and Laxemar – eastern Småland, south-eastern Sweden. SSM report 2010:40, Swedish Radiation Safety Authority.

**Beckholmen M, Tirén S A, 2010b.** Rock-block configuration in Uppland and the Ålands-hav basin, the regional surroundings of the SKB site in Forsmark, Sea and land areas, eastern Sweden. SSM report 2010:41, Swedish Radiation Safety Authority.

**Bergman S, Karis L, Söderman J, 2005.** Bedrock map 13H Gävle NO, scale 1:50 000. K 33, Sveriges geologiska undersökning.

**Bergman S, Stephens M B, Andresson J, Kathol B, Bergman T, 2012.** Sveriges berggrund, skala 1:1 miljon. K 423, Sveriges geologiska undersökning. (In Swedish.)

**Bingen B, Andersson J, Söderlund U, Möller, C, 2008.** The Mesoproterozoic in the Nordic countries. Episodes 31, 29–34.

**Carlsson A, 1979.** Characteristic features of a superficial rock mass in southern central Sweden: horizontal and subhorizontal fractures and filling material. Uppsala: Societas Upsaliensis pro geologia quaternaria. (Striae 11)

**Cederbom C, 2001.** Phanerozoic, pre-Cretaceous thermotectonic events in southern Sweden revealed by fission track thermochronology. Earth and Planetary Science Letters 188, 199–209.

**Curtis P, Wahlgren C-H, Bergman S, Antal Lundin I, Mellqvist C, Luth S, Olsson S, 2018.** 3D-modell över litotektoniska enheter och regionala deformationszoner i Sveriges berggrund. SGU-rapport 2018:05, Sveriges geologiska undersökning. (In Swedish.)

**Elming S-Å, Mattsson H, 2001.** Post Jotnian basic Intrusions in the Fennoscandian Shield, and the break up of Baltica from Laurentia: a palaeomagnetic and AMS study. Precambrian Research 108, 215–236.

**ESRI, 2017.** ArcGIS Desktop: Version 10.5.1.7333. Redlands, CA: Environmental Systems Research Institute.

**Gorbatshev R, 1967.** Petrology of Jotnian rocks in the Gävle area, east central Sweden. Stockholm: Sveriges geologiska undersökning. (Serie C 621)

**Hall A M, Goodfellow B W, Heyman J, Moon S, Caffee M W, Ebert K, Hättestrand C, Krabbendam M, Martel S J, Näslund J-O, Perron T, Stuart F M, Stroeven A P, 2018.** Glacial erosion of the Sub-Cambrian Peneplain in Sweden. EGU General Assembly Conference Abstracts 20, EGU2018-13835-1.

**Hall A M, Ebert K, Goodfellow B W, Hättestrand C, Heyman J, Krabbendam M, Moon S, Stroeven A P, 2019.** Past and future impact of glacial erosion in Forsmark and Uppland, Sweden. SKB TR-19-07, Svensk Kärnbränslehantering AB.

- Hermansson T, Stephens M B, Corfu F, Andersson J, Page L, 2007.** Penetrative ductile deformation and amphibolite-facies metamorphism prior to 1851 Ma in the western part of the Svecofennian orogen. *Fennoscandian Shield. Precambrian Research* 153, 29–45.
- Hobbs W H, 1903.** Lineaments of the Atlantic border region. *Geological Society of America Bulletin* 15, 483–506.
- Hobbs W H, 1912.** *Earth features and their meaning.* New York: Macmillan.
- Högdahl K, Sjöström H, Bergman S, 2009.** Ductile shear zones related to crustal shortening and domain boundary evolution in the central Fennoscandian Shield. *Tectonics*, 28, TC1003. doi:10.1029/2008TC002277
- Johansson M, 1999.** Analysis of digital elevation data for palaeosurfaces in south-western Sweden. *Geomorphology* 26, 279–295.
- Lagerbäck R, Sundh M, Svedlund J-O, Johansson H, 2005.** Forsmark site investigation. Searching for evidence of late- or postglacial faulting in the Forsmark region. Results from 2002–2004. SKB R-05-51, Svensk Kärnbränslehantering AB.
- Larson S-Å, Tullborg E-L, Cederbom C, Stiberg J-P, 1999.** Sveconorwegian and Caledonian foreland basins in the Baltic Shield revealed by fission-track thermochronology. *Terra Nova* 11, 210–215.
- Leijon B (ed), 2005.** Forsmark site investigation. Investigations of superficial fracturing and block displacements at drill site 5. SKB P-05-199, Svensk Kärnbränslehantering AB.
- Lidmar-Bergström K, 1994.** Berggrundens ytformer. In Fredén C (ed). *Sveriges Nationalatlas, Berg och jord.* Stockholm: Sveriges nationalatlas, 44–54. (In Swedish.)
- Lidmar-Bergström K, 1995.** Relief and saprolites through time on the Baltic Shield. *Geomorphology* 12, 45–61.
- Lidmar-Bergström K, 1996.** Long term morphotectonic evolution in Sweden. *Geomorphology* 16, 33–59.
- Lidmar-Bergström K, Olvmo M, 2015.** Plains, steps, hilly relief and valleys in northern Sweden – review, interpretations and implications for conclusions on Phanerozoic tectonics. Uppsala: Sveriges geologiska undersökning. (Research paper C 838)
- Lönnqvist M, Hökmark H, 2013.** Approach to estimating the maximum depth for glacially induced hydraulic jacking in fractured crystalline rock at Forsmark, Sweden. *Journal of Geophysical Research: Earth Surface* 118, 1777–1791.
- Malehmir A, Dahlin P, Lundberg E, Juhlin C, Sjöström H, Högdahl K, 2011.** Reflection seismic investigations in the Dannemora area, central Sweden: Insights into the geometry of polyphase deformation zones and magnetite-skarn deposits. *Journal of Geophysical Research: Solid Earth* 116, B11307. doi:10.1029/2011JB008643
- Martel S J, 2017.** Progress in understanding sheeting joints over the past two centuries. *Journal of Structural Geology* 94, 68–86.
- Martin C D, 2007.** Quantifying in situ stress magnitudes and orientations for Forsmark. Forsmark stage 2.2. SKB R-07-26, Svensk Kärnbränslehantering AB.
- Moon S, Perron J T, Martel S J, Holbrook W S, Clair J St, 2017.** A model of three-dimensional topographic stresses with implications for bedrock fractures, surface processes, and landscape evolution. *Journal of Geophysical Research: Earth Surface* 122, 823–846.
- Munier R, Talbot C J, 1993.** Segmentation, fragmentation and Jostling of cratonic basement in and near Äspö, southeast Sweden. *Tectonics* 12, 713–727.
- Nyberg J, 2016.** Marine geological map Södra Bottenhavet, sea bed sediments. K 541, Sveriges geologiska undersökning.
- Nyberg J, Bergman S, 2012.** Marine geological map Eggegrund-Gävle, geological sections. K 412:2, Sveriges geologiska undersökning.



- Näslund J-O (ed), 2010.** Climate and climate-related issues for the safety assessment SR-Site. SKB TR-10-49, Svensk Kärnbränslehantering AB.
- Olvmo M, 2010.** Review of denudation processes and quantification of weathering and erosion rates at a 0.1 to 1 Ma time scale. SKB TR-09-18, Svensk Kärnbränslehantering AB.
- Persson K S, Sjöström H, 2003.** Late-orogenic progressive shearing in eastern Bergslagen, central Sweden. *GFF* 125, 23–36.
- Philip G M, Watson D F, 1982.** A precise method for determining contoured surfaces. *Australian Petroleum Exploration Association Journal* 22, 205–212.
- Rudberg S, 1960.** Geology and morphology. In Sømme A (ed). *A geography of Norden*. Oslo: J.W. Cappelens forlag.
- Saintot A, Stephens M B, Viola G, Nordgulen Ø, 2011.** Brittle tectonic evolution and paleostress field reconstruction in the southwestern part of the Fennoscandian Shield, Forsmark, Sweden. *Tectonics* 30, TC4002. doi:10.1029/2010TC002781
- Sandström B, Page L, Tullborg E-L, 2006.** Forsmark site investigation.  $^{40}\text{Ar}/^{39}\text{Ar}$  (adularia) and Rb-Sr (adularia, prehnite, calcite) ages of fracture minerals. SKB P-06-213, Svensk Kärnbränslehantering AB.
- Sandström B, Tullborg E-L, Larson S Å, Page L, 2009.** Brittle tectonothermal evolution in the Forsmark area, central Fennoscandian Shield, recorded by paragenesis, orientation and  $^{40}\text{Ar}/^{39}\text{Ar}$  geochronology of fracture minerals. *Tectonophysics* 478, 158–174.
- Sederholm J J, 1897.** Om inledningen af prekambrika formationerna i Sverige och Finland och om nomenklaturen för dess äldsta bildningar. *Geologiska Föreningens i Stockholm Förhandlingar* 19, 20–53.
- Stephens M B, 2010.** Forsmark site investigation. Bedrock geology – overview and excursion guide. SKB R-10-04, Svensk Kärnbränslehantering AB.
- Stephens M B, Wahlgren C-H, 2008.** Bedrock evolution. In Söderbäck B (ed), *Geological evolution, palaeoclimate and historical development of the Forsmark and Laxemar-Simpevarp areas. Site Descriptive Modelling. SDM-Site*. SKB R-08-19, Svensk Kärnbränslehantering AB, 25–88.
- Stephens M B, Fox A, La Pointe P, Simeonov A, Isaksson H, Hermanson J, Öhman J, 2007.** Geology Forsmark. Site descriptive modelling Forsmark stage 2.2. SKB R-07-45, Svensk Kärnbränslehantering AB.
- Stephens M B, Ripa M, Lundström I, Persson L, Bergman T, Ahl M, Wahlgren C-H, Persson P-O, Wickström L, 2009.** Synthesis of the bedrock geology in the Bergslagen region, Fennoscandian Shield, south-central Sweden. Uppsala: Sveriges geologiska undersökning. (Serie Ba 58)
- Stephens M B, Follin S, Petersson J, Isaksson H, Juhlin C, Simeonov A, 2015.** Review of the deterministic modelling of deformation zones and fracture domains at the site proposed for a spent nuclear fuel repository, Sweden, and consequences of structural anisotropy. *Tectonophysics* 653, 68–94.
- Söderberg, P., and Hagenfeldt, S.E. (1995).** Upper Proterozoic and Ordovician submarine outliers in the archipelago northeast of Stockholm, Sweden. *GFF* 117, 153-161.
- Söderbäck B (ed), 2008.** Geological evolution, palaeoclimate and historical development of the Forsmark and Laxemar-Simpevarp areas. Site descriptive modelling. SDM-Site. SKB R-08-19, Svensk Kärnbränslehantering AB.
- Tirén S A, 2010.** Lineament interpretation Short review and methodology. SSM report 2010:33, Swedish Radiation Safety Authority.
- Tirén S A, Beckholmen M, 1989.** Block faulting in southeastern Sweden interpreted from digital terrain models. *Geologiska Föreningen i Stockholm Förhandlingar* 111, 171–179.
- Tirén S A, Beckholmen M, 1992.** Rock block map analysis of southern Sweden. *Geologiska Föreningen i Stockholm Förhandlingar* 114, 253–269.

**Twiss R J, Moores E M, 2007.** Structural geology. 2nd ed. New York: Freeman.

**Winterhalter B, 1972.** On the geology of the Bothnian Sea, an Epeireic Sea that has undergone Pleistocene Glaciation. Otaniemi: Geological Survey of Finland. (Bulletin 258)

**Öhrling C, Peterson G, Mikko H, 2018.** Detailed geomorphological analysis of LiDAR derived elevation data, Forsmark. Searching for indicatives of late-and postglacial seismic activity. SKB R-18-10, Svensk Kärnbränslehantering AB.



SKB is responsible for managing spent nuclear fuel and radioactive waste produced by the Swedish nuclear power plants such that man and the environment are protected in the near and distant future.

**skb.se**